Advanced Healthcare Materials

ADVANCED HEALTHCARE MATERIALS
www.advhealthmat.de

REVIEW OPEN ACCESS

Optoelectrical Devices for Neural Interfacing: Engineering Integration, Stability, and Multimodal Sensing

Stella Aslanoglou[1] | Barbara Spagnolo[1] | Antonio Balena[1,2] | Massimo De Vittorio[1,3,4] | Ferruccio Pisanello[1]

[1]Center for Biomolecular Nanotechnologies, Istituto Italiano di Tecnologia, Arnesano, Lecce, Italy | [2]Laboratoire Kastler Brossel, Sorbonne University, CNRS, ENS-PSL University, Collège de France, Paris, France | [3]Dip. di Ingegneria dell'Innovazione, Università del Salento, Lecce, Italy | [4]IDUN section, Dept. of Health Technology, Technical University of Denmark, Lyngby, Denmark

Correspondence: Ferruccio Pisanello (ferruccio.pisanello@iit.it)

Received: 30 September 2025 | **Revised:** 27 February 2026 | **Accepted:** 4 March 2026

Keywords: foreign body response | multifunctional neural interfaces | neurochemical sensing | optoelectrical devices | optoelectrical integration

ABSTRACT

In recent years, implantable optoelectrical devices have emerged as an effective resource for modulating and monitoring neural activity with high spatiotemporal resolution. By integrating optical stimulation, electrophysiological recording, and neurochemical sensing, these multifunctional interfaces offer novel ways to interrogate brain circuits in vivo. However, the greater the integration, the more sophisticated and consequently challenging the front-end of the implantable system becomes. The challenge revolves around three bottlenecks: (i) complexity of high-density optoelectrical integration, (ii) adverse long-term foreign body response (FBR), and (iii) limited incorporation of sensors for both cellular and biomolecular activity, including neurotransmitter activity and dynamics. Here we focus on the strategies to address these challenges in the context of device engineering at its interface with tissue. First, we present platforms developed by the scientific community for interacting with neural cells via electrical and optical means to achieve high resolution. Then we discuss soft, biocompatible materials and thermally-drawn polymer fibers to minimize mechanical mismatch and implementation of electrochemical, optical, and organic transistor-based sensors for multimodal neurochemical detection. Finally, we outline future perspectives for the development of next-generation neural interfaces capable of chronic, multisite, and multimodal interrogation of neural dynamics, with potential applications in both basic neuroscience and translational neurotechnologies.

1 | Introduction

Understanding the dynamic and multifaceted nature of brain activity is essential for advancing our knowledge of neural functions, clearing the path for innovative diagnostic and therapeutic strategies. To address this challenging task, the neuroscience community needs to be constantly fueled by new tools and technologies that can facilitate monitoring and modulation of neural activity at both single-cell and population-wide level. One of the most diffused approaches to unveil neural communication relies on the use of microelectrode arrays (MEAs), employing capacitive coupling to bi-directionally interact with nerve cells [1]. Because of the limited capacity of MEA-based studies to link the recorded activity patterns to cell-specific anatomical wiring [2], the earliest years of the 21st century witnessed the rise of genetically engineered optical tools to control and monitor neural activity. By expressing light-sensitive ion channels or pumps in specific neuronal classes [3], optogenetic actuators have enabled stimulation and inhibition of neural activity at the millisecond temporal scale with cell-type specificity. On

Massimo De Vittorio and Ferruccio Pisanello are co-last authors.

the other hand, genetically-encoded fluorescence indicators—proteins able to change their fluorescence in response to a specific biochemical change—have introduced the capability to optically monitor calcium dynamics, neurotransmitter concentrations as well as membrane voltage changes [4–6]. In addition, genetically-encoded sensors and actuators can be employed simultaneously for wavelength-multiplexed all-optical control and monitoring of neural activity [7, 8]. On the other hand, label-free Raman spectroscopy can identify physiological versus pathological tissue [9] providing simultaneous information for a wide range of tissue constituents.

These optical methods, with their unique advantages, are now widely recognized as complementary to electrical recordings, which remain central to neuroscience. Indeed, integrating recording pads into optical neural probes enables concurrent access to both high- and low-frequency (> 30 Hz and 0.5–30 Hz respectively) activity, the latter still inaccessible to purely optical methods. Moreover, modern implantable MEAs can incorporate thousands of passive or active recording sites [10, 11], providing dorso–ventral resolution and extent, unmatched by current optical techniques, along with the potential for on-board computation. Taken together, these advances underscore that optical and electrical techniques are not competing but synergistic, and their convergence has fostered the emergence of multifunctional opto-electrical neural interfaces. Over the past decade, this field has seen rapid progress, with increasingly sophisticated implantable platforms developed for optogenetics, electrophysiology, neurochemical sensing, and optical recording. In this landscape of signals generated from different physical means, it seems unrealistic to expect that observing one of them at a time could provide a comprehensive analysis of brain physiological and pathological states. Extensive literature has indeed demonstrated that integrative technologies combining high-throughput and multi-modal capabilities are needed [12, 13]. In this regard, multimodal experiments are crucial for causal investigations of neural circuits and for correlating signals and patterns at single-cell or population level [14]. The multimodal approach ultimately enhances our understanding of brain dynamics and cognitive functions and underpins the development of brain-machine interfaces in closed-loop architectures [15]. Another important feature of multimodality is that it allows for cross-modal validation, which is critical for confirming that signals obtained from distinct modalities faithfully reflect the underlying neural dynamics [16]. Multimodality is also key for a comprehensive study of brain diseases, as many conditions cannot be fully captured or addressed through a single sensing modality. For instance, brain tumors can be identified and discriminated through Raman spectroscopy [17], but a complete understanding of electrical and neurochemical interaction between the peritumoral region and the nearby healthy tissue is essential to understand the behavior of the invasive front. A further example is provided by neurodegerative conditions, including Parkinson's disease (PD) and Alzheimer's disease (AD). Here, multifactoriality is the shared trait between two of the most socially impactful neurodegenerative diseases, both affecting motor and cognitive capabilities. In particular, AD is caused by several interplaying factors including genetic traits, neuroinflammatory events, self-assembly of tau proteins, oxidative stress and cholinergic loss in multiple brain regions [18]. The etiology of PD, from the other hand, is linked to genetics, mitochondrial dysfunction, glial inflammatory states, dopamine (DA) imbalance and alpha-synuclein accumulation [19], while both AD and PD feature impaired calcium homeostasis and electrical signaling. The study of the numerous factors involved in disease onset and progression, with AD and PD representing only two of the most widely investigated diseases, can greatly benefit from the development of optoelectrical multimodal devices. These platforms combine optical and electrical modalities that interact with tissue to gather multiple disease-related biomarkers. The higher the level of device integration, the greater its potential to gather and correlate key players in the etiopathogenesis of multifactorial diseases with high spatio-temporal resolution. This capability is difficult to achieve when using multiple devices to correlate different types of physiological signals. Therefore, such multimodal systems can generate extensive and heterogeneous datasets offering unprecedented opportunities to probe neural dynamics from new perspectives, revealing how wiring, electrical and chemical activity contribute to the onset of the different and numerous brain functions and dysfunctions.

Yet, the integration of multiple modalities within a single device remains an open challenge [20]. In this review, we identify and describe three major challenges being addressed by the biomedical technology community in the front-end engineering of the implantable system (summarized in Figure 1), aimed at improving the interaction between electrical and optical physical means with neural cells. First, the challenge of optoelectrical integration density emerges from the need to match with the anatomic features of the brain region(s) of interest. This refers to the degree to which optical and electrical functional components can be miniaturized and densely co-integrated within a given area of a device, while maintaining independent addressability and reliable performance. Probing neural circuits with sufficient resolution requires dense arrays of recording, stimulation, and sensing elements that can simultaneously access large neuronal populations while preserving cellular-level specificity [21]. Yet, increasing integration density faces constraints related to device footprint, interconnection complexity, thermal dissipation, optical crosstalk, and signal integrity [22]. These trade-offs are broadly encountered across implantable neural technologies and become pivotal in multimodal systems, where optical, electrical, and chemical components must coexist within tightly confined volumes. As a result, insufficient integration density can limit the scalability of neural interfaces and restrict their ability to adapt to the diverse architectures of different brain regions, capture distributed circuit dynamics or implement advanced control strategies.

The second challenge refers to long-term biocompatibility. This is rooted in the inevitable presence of foreign body response (FBR), which in chronic settings compromises signal quality and device longevity [23]. Addressing compelling questions related to learning, plasticity, disease progression, and long-term therapeutic intervention, requires neural interfaces that operate reliably over extended periods. However, chronic implantation exposes devices to a complex biological environment characterized by mechanical motion, adverse immune responses, and biochemical degradation [24]. Mechanical mismatch between rigid devices and soft neural tissue, inflammatory responses, and gradual material failure can all degrade performance, leading to signal drift, loss of functionality, or device failure. These issues highlight the quest for a balance between sophisticated functionality, long-

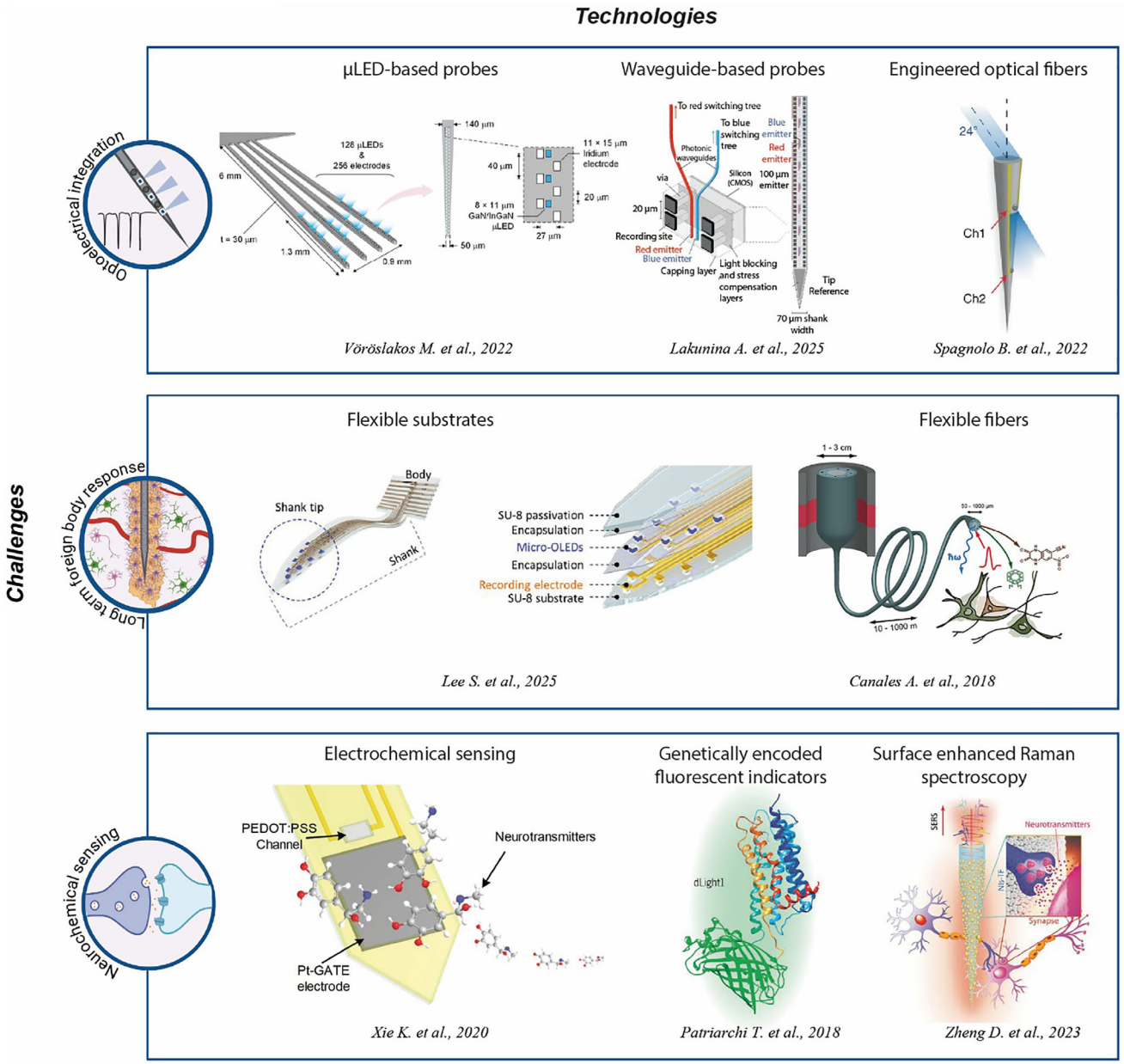

FIGURE 1 | Schematic overview of the structure of the review. The three main challenges faced by implantable optoelectrical devices for neural interfacing and the technologies that have been developed in response. Top panel (left to right): Reproduced under terms of the CC-BY license [30]. Copyright 2022, Wiley-VCH GmbH; Reproduced under terms of the CC-BY-NC-ND 4.0 International license [31]. Copyright 2025, Lakunina et al., bioRxiv; Reproduced with permission [32]. Copyright 2022, The Authors, under exclusive license to Springer Nature Limited. Middle panel (left to right): Reproduced under terms of the CC-BY-NC-ND 4.0 International license [33]. Copyright 2025, Wiley-VCH GmbH; Reproduced with permission [34]. Copyright 2018, American Chemical Society. Bottom panel (left to right): Reproduced under terms of the CC-BY license [35]. Copyright 2020, Xie et al.; Reproduced with permission [5]. Copyright 2018, The American Association for the Advancement of Science; Reproduced under terms of the CC-BY-NC 4.0 license [36]. Copyright 2023, Wiley-VCH GmbH. Created in https://BioRender.com.

term biocompatibility and mechanical compliance of the devices. This quest is particularly pronounced in multifunctional systems, due to their intrinsic need to host multiple types of materials with different mechanical, electrical, optical, and biochemical properties.

Finally, the integration of neurochemical sensing represents a third critical challenge that has emerged as the community increasingly recognizes the limitations of relying solely on electrophysiological and optical readouts to describe brain function. While these techniques provide high temporal and spatial resolution, they offer limited access to chemical signaling processes—such as neurotransmitter release, neuromodulation, ionic fluxes, and metabolic dynamics—that critically shape neural computation and network states. However, incorporating neurochemical sensors introduces substantial challenges, including achieving sufficient sensitivity and selectivity, ensuring long-term stability in vivo, and minimizing interference with co-located optical and electrical modalities [25]. Consequently, effective integration of neurochemical sensing remains a central and unresolved

challenge in the development of truly comprehensive and multifunctional neural interfaces. Addressing these points would be beneficial for better understanding several brain diseases (including brain tumors, neurodegeneration, and oxidative stress events) characterized by imbalances of neurochemicals [26], underscoring the need to directly monitor chemical dynamics in the brain. This growing awareness has driven efforts to integrate neurochemical sensing into multimodal neural interfaces to achieve a more complete and mechanistic understanding of both healthy and diseased brain function.

The aforementioned challenges have been distilled through the comparative analysis of recent technological advances in the field and serve as the organizational framework of this review. Beyond those challenges—strictly associated with the device front-end—it is important to acknowledge that next-generation neural interfaces are also subject to broader system-level constraints and requirements. These include power consumption, wireless powering, data communication, and packaging as well as closed-loop control and on-chip processing. While a detailed engineering discussion of these back-end aspects lies beyond the scope of this review, recognizing their role is essential, as their interplay with device-level innovations ultimately determines the robustness, scalability, and translational prospects of neural interfaces. Readers interested in an in-depth analysis of these complementary aspects are encouraged to consult recent reviews focusing specifically on wireless neural interfaces, power-efficient implantable systems, and closed-loop neuromodulation architectures [27–29].

2 | Challenges and Perspectives of Implantable Optoelectrical Neural Interfaces

2.1 | Optoelectrical Integration

Although the past decade has witnessed significant progress in large-scale neural recordings, with passive probes like the NeuroNexus—Buzsáki probe reaching up to 256 electrodes [37] and active probes like Neuropixels 2.0 [38] integrating as many as 5 120 channels, these levels of integration remain out of reach for optoelectrical devices [21]. Implantable optrodes—devices that combine optical stimulation or inhibition with simultaneous neural recording—still face two major challenges: (i) achieving a one-to-one correspondence between recording and light-delivery sites while maximizing their number, and (ii) minimizing the physical separation between stimulation and recording sites to enable higher spatial resolution and density. With these challenges in mind, in the following section we summarize the main technologies to integrate light emitting elements on implantable probes and the latest achievements in terms of integration density.

Light delivery sites are typically integrated onto stiff implantable shafts using either micro light-emitting diodes (μLEDs) or planar optical waveguides. μLEDs can be designed in a variety of geometries and are usually integrated via two approaches: "pick-and-place" and monolithic integration. In the case of the "pick-and-place" approach, μLEDs originally produced in a donor substrate such as silicon or sapphire are transferred to the implantable shaft [39]. The transfer consists in first releasing the donor substrate via laser lift-off, mechanical grinding or wet etching and in a second step picking and placing the μLEDs on the desired positions on the shaft via transfer printing using an elastomeric stamp or capillary bonding. Once the assembly is completed, interconnections of μLEDs are realized [40]. "Pick-and-place" is a reliable technique that ensures precise positioning of the μLEDs on the final device in a high throughput manner and has been extensively employed in the fabrication of μLED arrays for optrodes [41]. However, it is limited to a relatively large size of μLEDs (> ∼ 50 μm). In the case of monolithic integration—an approach originally introduced by Wu et al. [42]—material growth and device preparation are all performed on the same wafer, thus allowing for the co-integration of μLEDs and their respective electronic circuits directly in the implantable shaft. This is a highly scalable approach that gained popularity over the last years leading to the realization of high-density μLED arrays [43], and it is in principle, compatible with the integration of nearby photodetectors [44] to further extend sensing modalities. Notably, monolithic integration of organic LEDs (OLEDs) for optogenetic stimulation probes has also been demonstrated recently [45]. Despite their high versatility, μLED-based probes are subjected to thermal management issues due to the heat dissipation generated during the operation of the μLEDs and their active electronics [46].

Planar optical waveguides are instead flat, slab-like structures able to confine and guide light along a defined path with minimal loss. Their operation is based on dielectric confinement of light, where visible electromagnetic radiation propagates within a high refractive index medium (n_1) surrounded by a lower refractive index material ($n_1 > n_2$). Optical waveguides are typically fabricated using semiconductors (e.g. Si and SiN) and polymers (e.g. SU-8 and polymethyl methacrylate (PMMA)), and depending on their size can carry either a single or a few modes at specific wavelengths. Microscale waveguides are fully compatible with microfabrication techniques and as a result can be directly integrated into the implantable shaft, while light is usually edge-coupled using an optical fiber [47] and delivered into the brain at high efficiency by using out-coupling elements based on diffraction gratings [48] or phased arrays [49]. Therefore, unlike μLEDs, optical waveguides are entirely passive, avoiding heat generation issues.

Both μLEDs and integrated optical waveguides can be combined with electrodes for extracellular recordings, enabling simultaneous optogenetic stimulation and electrophysiological monitoring. However, as integration density increases, light-emitting elements and recording electrodes must unavoidably be positioned in close proximity. This serves the dual purpose of maximizing the number of functional sites and ensuring optimal spatial overlap between stimulation and detection volumes. Yet, such close integration renders these systems susceptible to optical-stimulation-induced artifacts, primarily arising from the Photovoltaic (PV) effect, also known as the Becquerel effect [50, 51], and the electromagnetic interference (EMI) effect [52]. The PV effect consists in the generation of photocurrents at the electrode–electrolyte interface upon light exposure and is relevant for both μLED and waveguide-based optrodes, while EMI results from capacitive or inductive coupling between the light-driving circuits and the recording channels and therefore is observed only for the μLED technology. Those types of artifacts, rising mostly at the onset and offset of the light pulse, risk to obscure the underlying

neuronal signals and consequently compromise the temporal resolution of the optrode. Depending on the technology used to fabricate the device, different approaches have been developed to minimize those artifacts, enhancing signal-to-noise ratio (SNR) and often unveiling the entire neural electrical activity.

A notable recent advancement in this context is the "miniSTAR" (minimal-stimulation-artifact) μLED optrode developed by Kim et al. [53]. This device integrates 128 recording electrodes and 32 independently addressable μLEDs on a single shank (Figure 2a), enabling high-resolution opto-electrophysiology. To suppress optical-stimulation-induced artifacts, the "miniSTAR" design implements several key innovations. A triple-metal-layer interconnect scheme was introduced to spatially separate the optical drive lines from the recording traces, significantly reducing EMI. Additionally, a dedicated shielding layer was placed between stimulation and recording interconnects to further block capacitive coupling. To minimize the PV effect, which arises from photoinduced charge generation at the silicon–electrolyte interface, the authors employed a heavily boron-doped silicon substrate. This doping reduces the minority carrier lifetime, thereby suppressing the generation of photoelectric artifacts (Figure 2b,c). Collectively, these architectural and material optimizations enable artifact-free, high-temporal resolution recording of neuronal activity during optical stimulation. The same group, later on, expanded on this approach and developed the "HectoSTAR" optrode [30], featuring two times the number of recording and four times the number of stimulation sites of that of the "miniSTAR" – 256 recording electrodes and 128 stimulation μLEDs in a single probe—achieving a threefold increase in spatial density without compromising either recording fidelity or optical output (Figure 2d). This was made possible through further miniaturization of the μLEDs and optimization of circuit layout to maintain low noise and minimal heat dissipation despite the increased channel count. As a result, "HectoSTAR" enabled the performance of multi-region (such as neocortex and hippocampus or CA1 and CA3 hippocampal subregions) high-density recordings together with high-precision optogenetic stimulation deep in the brain.

While the mitigation strategies implemented in miniSTAR and HectoSTAR effectively suppress light-induced artifacts, they remain subject to several important limitations. Their performance is closely tied to specific electrode materials, surface treatments, and electrolyte environments, raising concerns about transferability to other optoelectrical devices. Different electrode materials—including gold, platinum or carbon-based (e.g. carbon nanotubes (CNT) and graphene)—and coatings such as PEDOT:PSS, exhibit distinct photoelectric cut-off thresholds, which determine the light intensity at which artifacts are generated [54]. Materials with lower thresholds generate artifacts at lower light intensities, thus necessitating thicker shielding, which can compromise the mechanical compliance of the device. In this context, serpentine-shaped shielding metal layers are advantageous as they can provide effective artifact suppression while preserving mechanical compliance through increased flexibility [55]. At the same time, electrolyte variations—including ionic strength, concentration and pH—can modulate charge transfer and ionic flow at the electrode surface [56]. Consequently, an artifact mitigation strategy performing well in PBS in vitro may not be that effective in a physiological environment in vivo. In addition, the reported artifact suppression is demonstrated under specific optical stimulation regimes. Strategies that rely on shielding, differential signal paths, or temporal filtering may be robust under low-duty-cycle or pulsed illumination, but their efficacy can degrade under higher duty cycles or increased stimulation frequencies. In particular, higher-duty-cycles (more time ON during each stimulation cycle) imply more total illumination that consequently generates larger artifacts. Similarly, higher stimulation frequencies can induce artifact build-up by preventing complete decay of artifact waveforms, promoting temporal overlap, and increasing spectral interference with neural signals [50]. Therefore, direct extrapolation of reported results to other stimulation paradigms should be approached cautiously. Finally, scalability of these approaches to higher-density systems also presents a challenge. In particular, as array density increases and cross-sectional footprint is further reduced—particularly in the context of 3D stacking—the available area for shielding structures and routing separation diminishes. In such regimes, maintaining effective EMI suppression and isolation, as implemented in miniSTAR and HectoSTAR, becomes increasingly challenging due to routing congestion, interlayer coupling, and discontinuities in shielding across stacks.

Another frontier for optrodes is the capability of allowing for dual-color optogenetics, opening up new possibilities for modulating multiple cellular functions at the same time or optotagging two genetically defined neural populations in parallel [57]. From the neural implant's perspective, the challenge lies in the compact integration of dual-light sources and a high-density recording system. Ko et al. recently reported on a dual-color μLED integrated neural probe allowing for multi-control optogenetic electrophysiology [58]. This dual-color probe, termed "DuoLite", was realized in two steps: first by fabricating a polyimide (PI)-based flexible probe incorporating red (λ_{peak} = 647 nm) μLEDs and second by stacking this probe onto a silicon-based blue (λ_{peak} = 463 nm) μLED optrode (Figure 2e). The versatility of the fabrication process followed here allows customizing the size and spacing of μLEDs and recording sites depending on the experimental needs.

Unlike μLEDs, semiconductor waveguides are typically coupled with passive photonic structures such as gratings or ring resonators to shape and direct light emission, thereby helping to mitigate undesired optical-stimulation-induced artifacts [59]. By precisely controlling the emission angle and location, these outcouplers minimize direct illumination of the recording electrodes, which is a key source of photoelectric and photovoltaic artifacts. Additionally, since light is guided and emitted through dielectric materials rather than from on-chip active light sources, the risk of local heating and EMI effect is significantly reduced. Roszko et al. [60] recently demonstrated a Si photonic neural probe featuring 26 pairs of stimulating—recording sites able to perform dual-color photostimulation and electrophysiological recording (Figure 2f). Using on-shank directional-coupler wavelength demultiplexers and low crosstalk waveguide arrays a record of 52 emitters was achieved (Figure 2g). A further leap in optoelectrical integration has been achieved with the Neuropixels Opto probe [31], which combines the high-density recording capabilities of Neuropixels with on-chip photonic waveguides. In this architecture, red (638 nm) and blue (450 nm) laser light is generated off-shank—outside the

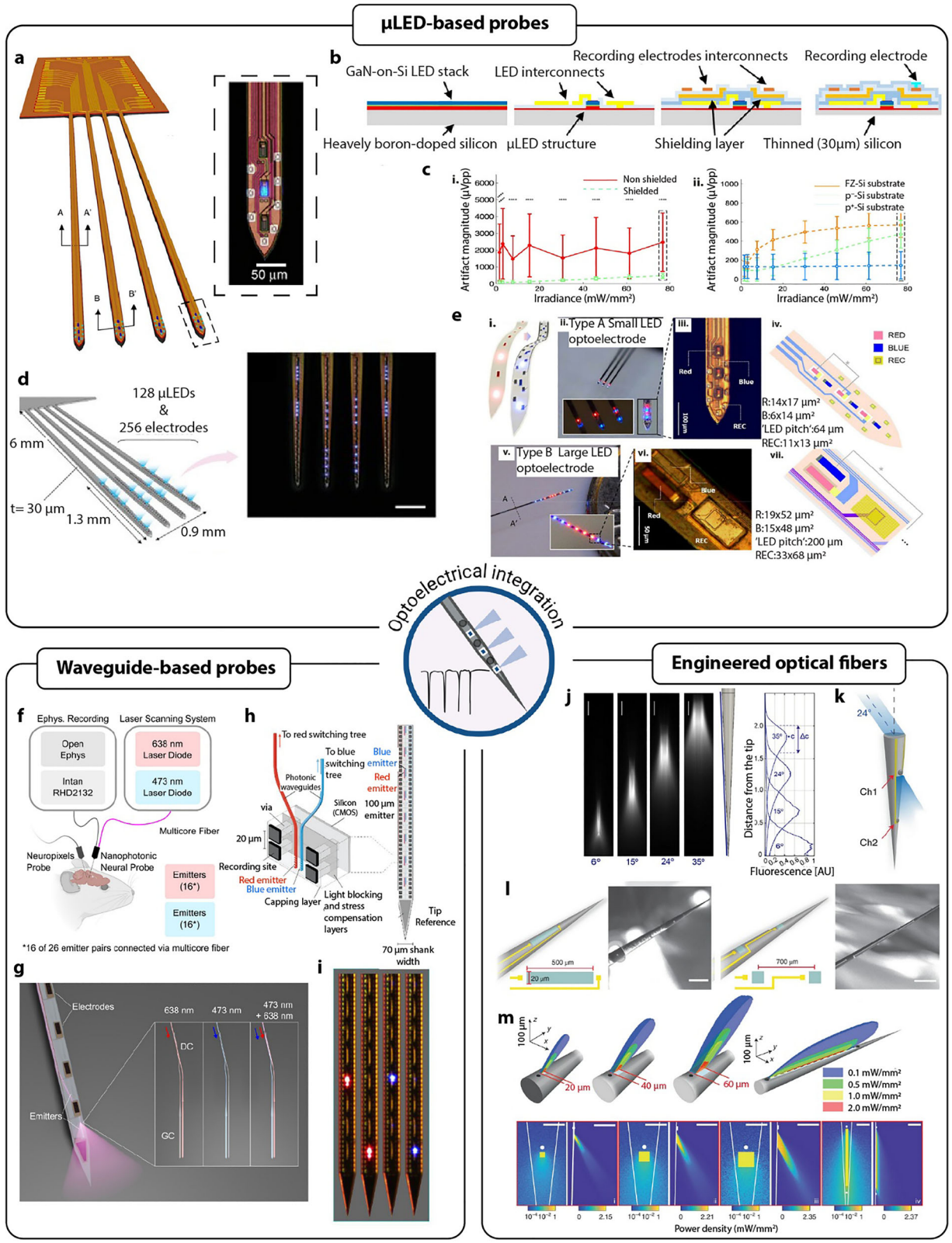

FIGURE 2 | Implantable optoelectrical neural probes. (a) Schematic illustration of the miniSTAR optrode. (b) Illustrative cross-section containing one µLED and one recording electrode showing the innovations employed in the fabrication process. (c) Reduced EMI and PV artifacts. (i) Comparison of mean peak-to-peak magnitudes of highpass filtered stimulation artifact recorded on the shielded (green) and the non-shielded (red) µLED optrodes. (ii) Comparison of the mean peak-to-peak magnitude of highpass filtered voltage signal recorded on shielded µLED optrodes with different substrate doping densities upon external light exposure. Reproduced under terms of the CC-BY license [53]. Copyright 2020, The Authors, Springer Nature. (d) Schematic illustration and microphotograph of a four-shank hectoSTAR µLED optrode containing a total of 128 µLEDs and 256 microelectrodes. Scale bar: 300 µm. Adapted under terms of the CC-BY license [30]. Copyright 2022, Wiley-VCH GmbH. (e) The DuoLite optrode. (i) Schematic illustration of

brain—and routed along the shank through integrated waveguides to programmable photonic emitters (Figure 2h,i). Avoiding on-shank light generation not only allows for higher optical powers without thermal constraints, but also prevents direct irradiation of recording electrodes. As a result, the Neuropixels Opto probe achieves artifact-minimized opto-electrophysiology while maintaining subcellular spatial control and high temporal resolution.

An effective alternative approach to implantable optoelectrical integration is represented by silica optical fibers. Standard multimode optical fibers are cylindrical optical waveguides with small diameter (50 – 200 μm) exhibiting excellent optical properties that have seen their first implementation in optogenetic stimulation in vivo dating back to 2007 [61]. Since then, they have been extensively used in conjunction with MEAs for simultaneous performance of optogenetic stimulation and electrophysiological recordings [62]. Nevertheless, they are gradually giving their place to engineered implantable waveguides like tapered optical fibers (TFs), which provide a highly versatile platform for simultaneous light delivery and neural recording, particularly in deep brain regions [32]. TFs are fabricated by gradually narrowing the diameter of a standard multimode optical fiber down to a few micrometers, creating a smooth, conical waveguide. Compared to their flat-cleaved counterparts, TFs are less invasive to the brain tissue and enable light delivery and collection across larger brain volumes [63]. In addition, this geometry allows for spatially resolved light emission along the taper through modal demultiplexing, where the angle of light injection into the fiber controls the axial outcoupling position (Figure 2j). This tunability enables selective activation of distinct brain regions using a single implant [63, 64], while customized emission sites can be obtained using microfabrication methods for non-planar surfaces including focused ion beam milling [65], laser ablation [66] or two-photon lithography [67, 68]. Light emitting sites can be paired with electrodes integrated along their non-planar surface, giving rise to hybrid optoelectrical devices known as "fibertrodes" [69] (Figure 2k,l). These devices combine high-precision optical stimulation with simultaneous extracellular recording while maintaining a small footprint and low invasiveness. Importantly, by controlling the emission angle and precisely positioning the optical windows and the electrodes on the base of tissue scattering properties (Figure 2m), fibertrodes minimize direct light exposure to the recording sites. This allows abating the PV effect below the threshold for unveiling action potentials elicited during optogenetic stimuli as short as 2 ms, which are temporal windows typically obscured due to the overlap with photoelectric artifacts at stimuli's onset and offset [32].

The need for interfacing with wider brain volumes has given rise to the development of fiber bundles. These consist in the assembly of multiple optical fibers able to deliver light to different brain areas simultaneously [70]. While single TFs target highly localized brain volumes for ultra-precise stimulation of small neuronal populations, fiber bundles allow distributed optogenetic stimulation across multiple cortical layers simultaneously. In this context, Eriksson et al. [51] bundled 10 ultrathin optical fibers of different lengths in a total diameter of < 80 μm, achieving axial stimulation distribution across a total range of 5 mm with 500 μm resolution. The fiber bundle was implanted adjacent to a silicon laminar probe generating a hybrid optrode. The implantation of six of those optrodes bilaterally in the mouse brain allowed for 3D optogenetic stimulation and laminar electrophysiological recordings across extended cortical layers.

It is evident that optoelectrical integration has made strong strides in recent years, driven by advancements in microfabrication and nanophotonics. Indeed, μLED-based optrodes have now achieved unprecedented integration densities allowing for modulation and recording with high spatiotemporal resolution and minimal artifacts. At the same time, dual-color photostimulation coupled with electrophysiology is now possible, opening up the way for more sophisticated investigations of brain functional connectivity. Moreover, the integration of passive photonic structures with semiconductor waveguides offers a compelling pathway for advancing artifact-free, high-density opto-electrophysiology and overcoming many of the limitations associated with μLEDs,

the stacking of the "red" and "blue" μLED probes. (ii) Bird's eye view of small-area targeting DuoLite. (iii) Expanded view of a single shank in (ii). (iv) Schematic illustration of the design of the stacked small-area targeting DuoLite depicted in (iii). (v) Bird's eye view of large-area targeting DuoLite. (vi) Expanded view of the shank shown in the inset of (v). (vii) Schematic illustration of the design of the stacked large-area targeting DuoLite depicted in (vi). Reproduced with permission [58]. Copyright 2024, Ko et al., bioRxiv. (f) Conceptual figure illustrating the simultaneous performance of dual-color photostimulation and electrophysiological recordings using the nanophotonic neural probe and a Neuropixels probe. (g) Graphical rendering of a dual-color nanophotonic neural probe. Each routing waveguide connects to a directional coupler, which demultiplexes red (638 nm) and blue (473 nm) light to separate grating coupler emitters. Reproduced under terms of the CC-BY license [60]. Copyright 2025, The Authors, SPIE. (h) Cross-section of the Neuropixels Opto probe, showing the TiN recording sites (connected with a "via" to the silicon CMOS layer) and the SiN photonic waveguides ending in the emitters (grating couplers). (i) Photos of a probe shank across four time points, with two red and two blue emitters delivering light in succession. Reproduced under terms of the CC-BY-NC-ND 4.0 International license [31]. Copyright 2025, Lakunina et al., bioRxiv. (j) Spatially selective light delivery using high-NA TF. Left: emission images for a 0.66 NA, 200 μm core size fiber with increasing input angle. Center: Diagram of the tapered section. The blue line indicates the profile along which the intensity was measured. Right: Intensity profiles measured at different input angles with respect to the distance from the tip. Reproduced under terms of the CC-BY license [64]. Copyright 2018, The Authors, Springer Nature. (k) Schematic illustration of a fibertrode featuring two electrodes and a rectangular slot-like aperture. (l) Sketches and SEM images of different fibertrode designs. Scale bar: 200 μm. (m) Top: Iso-intensity surface maps at 0.1, 0.5, 1, and 2 mW/mm^2 of the simulated light emission distribution for three different windows sizes and a rectangular slot. Bottom: Power density distributions for the three different windows sizes and the slot aperture at the fiber surface (left, normalized logarithmic colour map) and in a meridional plane cutting the aperture in two halves (right, linear colour map). Data are shown for an average power density of 2 mW/mm^2. White dots on the tapers represent the electrodes. Scale bars: 100 μm. Reproduced with permission [32]. Copyright 2022, The Authors, under exclusive license to Springer Nature Limited.

TABLE 1 | Comparative analysis between optoelectrical devices including key performance metrics.

Device Performance	Mini STAR [53]	Hecto STAR [30]	DuoLite [58]	Dual-color nanophotonic probe [60]	Neuropixels Opto [31]	Fibertrode [32, 69]
Max irradiance	50 mW/mm^2	0.6 mW/mm^2	Small Red: 50 mW/mm^2 Small blue: 120 mW/mm^2	25.6 mW/mm^2	10 mW/mm^2	Tens of mW/mm^2
Stimulation efficiency	Evokes spikes in CA1 neurons using 3 mW/mm^2	Multi-regional, 84 ± 28 single units/session	Red light: elicited spiking in 26/8 (30%) Pyr and in 1/1 (100%) interneurons; Blue light: increased firing rate from 19.96 Hz to 37.52 Hz in 1 putative unit	local activation of 11 units, spatial multiplexing	Activation of spatially separated neural populations; 96 units from 25 sessions (red light); 198 units from 26 sessions (blue light)	Dynamic light-delivery, spatially resolved recording of AP and LFP
Recording fidelity	High temporal resolution (< 1 ms)	Highextracellular spikes > 200 µV	Not reported	Locally evoked activation during red photostimulation; not regional activation	High	High extracellular spikes > 60 µV
Integration density	32 recording sites, 12 µLEDs	256 recording sites, 128 µLEDs	32 recording sites, 12 blue and red µLEDs	52 photonic channels, 26 recording sites	384 recording sites, 28 emitters (grating couplers)	2 recording sites, 2 optical windows
Thermal performance	Not reported	≤ 0.6°C rise in brain tissue	Not reported	≤ 0.15°C for max power density	Not reported	~0.1°C for a 20 × 20 µm optical window
Mechanical compliance	Low	Low	Low	Low	Low	Moderate
Max operating current	100 µA	75 µA	300/200 µA (large/small red) 300/100 µA (large/small blue)	N/A	N/A	N/A
Light-induced artifacts	Low < 50µVpp	removed before automatic spike sorting	red LED 1.88 ± 0.11 mV (onset) and 1.45 ± 0.09 mV (offset); blue LED (11.6 ± 0.4 µV (onset) and 9.9 ± 0.39 µV (offset)	Removed by a 10 ms blanking period, centered on each pulse onset and offset, applied for each stimulation pulse.	Low 5.4 ± 2.4 µV for AP and 5.3 ± 3.7 µV for LFP	Negligible

including thermal load and restricted optical output power. In parallel, fibertrodes represent a highly evolving class of optoelectrical devices for neural interfacing that is anticipated to enable closed-loop all-optical interrogation of neural circuits in the future, by virtue of their intrinsic compatibility with fluorescence collection in vivo. A comparative analysis between the optoelectrical devices discussed in the section is presented in Table 1 below. In particular, the table summarizes key performance metrics selected for describing important features related to the aforementioned devices. Parameters such as maximum irradiance values, stimulation efficiency, recording fidelity, integration density, thermal performance, mechanical compliance, maximum operating current and the presence of light-induced artifacts, are reported. The table highlights differences between devices, showcasing the recent advancements in the field. Moreover, it serves as a guide for selecting the most appropriate engineered optoelectrical tool tailored to the respective experimental needs including spatial selectivity and local or regional activation.

Looking forward, optoelectrical integration is expected to push the limits even further aiming to achieve one-to-one pairing between optical stimulation and electrical recording sites, potentially enabling new frontiers for single-cell opto-tagging. To this aim, future developments will likely focus on further miniaturization of components—both for LEDs and photonic circuit-based devices—as well as novel flexible and tissue-compliant materials (discussed in the next section). At the same time, 3D stacking fabrication approaches, consisting in the vertical integration of multiple functional layers in a single compact probe, will allow for a dramatic increase of integration density keeping a minimal device footprint, and for further

functionalities to be integrated. This includes the capability of sensing optical signals, which must coexist with light delivery to enable fluorescence generation. In the case of μLEDs and planar optical waveguides, this is being targeted by the introduction of photodetectors directly on the shaft, ideally as close as possible to the light delivery site. An example is represented by the work of Taal et al. [44], where single-photon avalanche photodiodes (SPADs) have been integrated into a neural probe underneath a diffraction grating acting as wavelength filters for incoming light radiation. In the case of fiber-optic based devices, transduction of photons is instead performed off-board, with the modal properties of the implanted dielectric system defining the light collection diagram. For instance, TFs can potentially enable wide-volume or depth-selective light delivery with simultaneous light collection capabilities and electrophysiological recording.

Of course, the higher the integration density and the number of integrated functionalities, the higher the amount and complexity of the collected data. In this context, the development of automatic algorithms, using deep learning methods, to cluster large datasets for reliable sorting and interpretation will be necessary [71]. Beyond clustering, the following analysis roadmap is recommended to guide real-time processing of multimodal signals for next-generation closed-loop systems:

i **Alignment**

Performance of multimodal spatio-temporal alignment aiming to resolve intrinsic mismatches across heterogeneous signals acquired at different spatial and temporal scales to ensure coherent interpretation of neural activity from single cell to networks [16].

ii **Art removal**

Use of stimulation-locked artifact suppression pipelines aiming to remove artifacts that overlap with physiological activity by combining hardware-level mitigation strategies with adaptive signal-processing and learning-based approaches, including template subtraction, component decomposition (e.g., ICA), targeted filtering, and deep learning–based denoising methods [72, 73].

iii **Integration**

Performance of multimodal feature fusion aiming to integrate complementary information from different modalities into unified representations using data-driven approaches, improving robustness and enabling cross-scale interpretation linking cellular, network, and behavioral dynamics [74].

iv **Real-time control**

Use of closed-loop decoding and estimation frameworks aiming to enable real-time extraction of relevant features, neural state estimation, and feedback-driven control within low-latency processing pipelines, supporting adaptive modulation across experimental conditions and datasets [75].

2.2 | Long Term Foreing Body Response

The implantation of any foreign material into the body triggers an inflammatory and fibrotic process known as FBR, which evolves through well-defined temporal stages [76]. In the case of tissue-penetrating neural probes, FBR is initiated at the moment of insertion, causing immediate tissue damage. This includes disruption of the blood–brain barrier (BBB), damage to blood vessels, and neuronal death in the vicinity of the implant [77]. Within hours to days, activated astroglia and microglia migrate to the injury site, where they proliferate and within the first weeks form a progressively thickening cellular sheath that insulates the probe. In particular, this progressive glial encapsulation and neuronal loss gradually increases interfacial impedance, reduces SNR and degrades the electrical, optical, and chemical interfacing performance of the probe leading to device failure [78]. In parallel, ongoing brain movements resulting from both physiological processes (e.g., respiration and heartbeat) and animal behavior cause relative displacement between the probe and the surrounding tissue, leading to cumulative mechanical damage at the implantation site [23]. Minimizing FBR is therefore critical to ensuring the long-term stability and functionality of implantable neural interfaces.

In this context, FBR induced by the implantation of optoelectrical devices is modulated by (i) device architectures and material choices that have a strong impact on mechanical damage [79], and (ii) the use of light that leads to tissue heating, thermally-induced damage and alteration of neural physiology [80]. From the material point of view, optoelectrical devices based on rigid substrates—such as glass or semiconductors (e.g. Si)—exhibit Young's Modulus that ranges between 70–170 GPa [23], implying a significant mechanical mismatch between them and the soft brain tissue, whose Young's modulus is in the range of 1–10 kPa [81]. This mismatch generates strain during brain micromotion, enhancing the local inflammatory response and consequent formation of glial scars that can alter device performances, with Si-based implants among the less advantageous, especially in a chronic setting. In a recent study, Villamarin-Ortiz and colleagues evaluated the acute biological response of cortical neurons to the implantation of a Utah array made of penetrating optical needles with different shapes and by applying different insertion forces (9-20 psi). Glial fibrillary acidic protein (GFAP) immunostaining quantification confirmed that higher insertion pressures lead to greater mechanical stress and that sharp geometry minimized astrocytic and microglia activation even in the case of 100 μm diameter shanks [82]. The shape-effect is also evident when comparing flat and taper-shaped optic fiber-based optoelectrical devices, with TFs strongly reducing FBR [63] due to their sharp, conical tips, which require less insertion force and consequently minimize tissue and vascular damage as well as glial response [83].

Conversely, neural implants based on soft and flexible substrates, including parylene-C, SU-8, and PI [84–86], are more tissue compliant and allow for small implantation footprints with reduced invasiveness. For instance, Guan et al. [86] demonstrated that PI encapsulation of 100-nm-thick Au microelectrodes enabled the fabrication of the Neurotassel; a platform featuring multiple ultra-flexible and self-arranging electrode bundles. This high mechanical compliance promoted seamless integration with the

surrounding tissue, resulting in long-term (over 5 weeks) recordings, with no significant SNR variations over time, indicative of sustained electrode-tissue coupling. However, light delivery was obtained by means of a diode laser coupled to an optic fiber rather than being integrated onto the device, thus increasing the brain area affected by the implant. Overall, long-term animal studies (up to 8 weeks post-implantation) have demonstrated that polymer-based probes elicit significantly lower levels of inflammatory biomarkers reducing chronic tissue stress and delaying the formation of insulating cellular sheaths, compared with their silicon-based counterparts [87].

Beyond mechanical and geometrical considerations, optoelectrical neural interfaces introduce distinct long-term interface challenges that are absent in purely electrical ones. In addition to mechanical mismatch, those systems face thermal cycling from μLEDs or OLEDs, optical component-induced stiffness and complex mechanical coupling in multilayer stacks, all of which can enhance chronic FBR. Periodic activation of μLEDs or OLEDs generates transient local temperature elevations, and although peak temperature rises may remain within conventional safety limits (< 1°C), compliance with this acute threshold alone does not necessarily ensure safety under repeated or chronic stimulation. Indeed, studies on thermal stress suggest that repeated sub-threshold heating can promote glial activation and neuroinflammatory responses [88]. These findings indicate that repeated exposure to dynamic, sub-threshold thermal loads may cumulatively perturb cellular homeostasis, even in the absence of overt temperature violations. Moreover, chronic optical stimulation may introduce phototoxic stress and reactive oxygen species (ROS) generation, further contributing to biological stress beyond purely thermal effects. Together, these considerations suggest that long-term and high-duty-cycle stimulation paradigms require careful optimization and management in order to avoid cumulative tissue stress [89]. Moreover, optical components often exhibit higher elastic moduli than surrounding polymer substrates, introducing localized stiffness gradients. Optoelectrical probes often come in multilayer architectures, where optical components, interconnects, electrodes and encapsulation layers are mechanically coupled, resulting in overall mechanical properties very different from the ones of the single materials [90]. In addition, differential strain accumulation across these heterogeneous layers during brain micromotion can induce interfacial delamination, localized stress amplification, or microfractures that progressively degrade both compatibility and performace of the device [91].

Maintaining compliance during multimodal integration is therefore a significant challenge for the field, since each additional functionality often requires materials or structures with distinct mechanical and thermal properties, which can reintroduce stiffness or volumetric bulk. Careful design strategies, including modular architectures, strain-isolated layers, and the use of composite or hybrid materials, are therefore essential to preserve soft-tissue compatibility and minimize FBR over chronic timescales.

One path followed by the neurotechnology community toward the realization of optoelectrical neural implants with minimal FBR is represented by the translation of μLED and micro-OLED technologies, described in the previous section, on flexible substrates. A recent example is that of 'flexLiTE' (Figure 3a), featuring 12 soma-sized individually addressed μLEDs and 32 recording microelectrodes fabricated by stacking together two PI-based probes: a stimulating 'LED' and a recording 'REC' probe (Figure 3b). By keeping a small footprint (12 μm thick and 115 μm wide shank) and distributing functional components laterally rather than vertically, flexLiTE limits local stiffness discontinuities that would otherwise concentrate strain during brain micromotion. This architectural strategy directly addresses a key driver of chronic FBR by reducing micromotion-induced shear stress at the tissue–device interface. As a result, flexLiTE exhibits improved long-term tissue compatibility that allows reliable performance of in vivo opto-electrophysiology in freely moving mice over a period of 8 months [92]. At the same time, Lee et al. [33] recently reported on the first flexible neural probe with integrated micro-OLEDs (Figure 3c) for localized high-resolution stimulation and electrical recording with minimal invasiveness. OLEDs offer several unique advantages for chronic neural interfacing, particularly in reducing FBR. Unlike inorganic μLEDs, which consist in crystalline layers, micro-OLEDs consist in plastic organic layers, which are thinner, lighter and more flexible. As a result, micro-OLEDs can be monolithically integrated on ultra-thin, flexible, and stretchable substrates, which significantly improves mechanical matching with brain tissue and minimizes micromotion-induced damage. Moreover, their inherently low thermal output reduces the risk of tissue overheating, while their planar, low-profile architecture allows seamless integration into soft implantable probes without increasing volume or stiffness. Furthermore, micro-OLEDs can be patterned at high spatial density using scalable manufacturing processes such as inkjet printing [93] or roll-to-roll fabrication [94], supporting customizable multi-site stimulation in compact formats. These properties make micro-OLEDs a promising platform for next-generation minimally invasive optoelectrical neural interfaces with reduced inflammatory response and improved long-term performance.

A complementary approach is instead represented by a technological platform destined directly for ultra-flexible multifunctional neural implants. It is based on polymer optical fibers (POFs) fabricated via the thermal drawing process (TDP) that have recently gained increased attention as they have set the stage for fully integrated and highly compliant optoelectrical neural interfaces [34]. TDP is a highly scalable technique that in its conventional version consists in gradually heating a macroscopic polymer preform above its glass transition temperature while stretching it using a fixed speed in order to produce a continuous and uniform fiber [95]. The type of polymer used determines the fiber's mechanical, optical and thermal properties. Typical polymers employed in TDP are thermoplastics including PMMA, polycarbonate (PC) and polysulfone (PSU) [96, 97]. Following the same concept, polymer preforms can be simultaneously fed with additional materials, such as metal microwires and carbon fibers (CF) [98] (Figure 3d,e) allowing for multimodal integration without adding significant volumetric bulk. In addition, the resulting fiber-based probes inherently adopt a cylindrical geometry, which promotes uniform stress distribution during brain micromotion preventing local tissue damage that would otherwise sustain inflammatory signaling and accelerate fibrotic encapsulation. Recently, Kim et al. used this co-drawing fabrication approach to produce a multifunctional probe for bidirectional synaptic probing [99] (Figure 3f). This fiber-based probe combines real-time

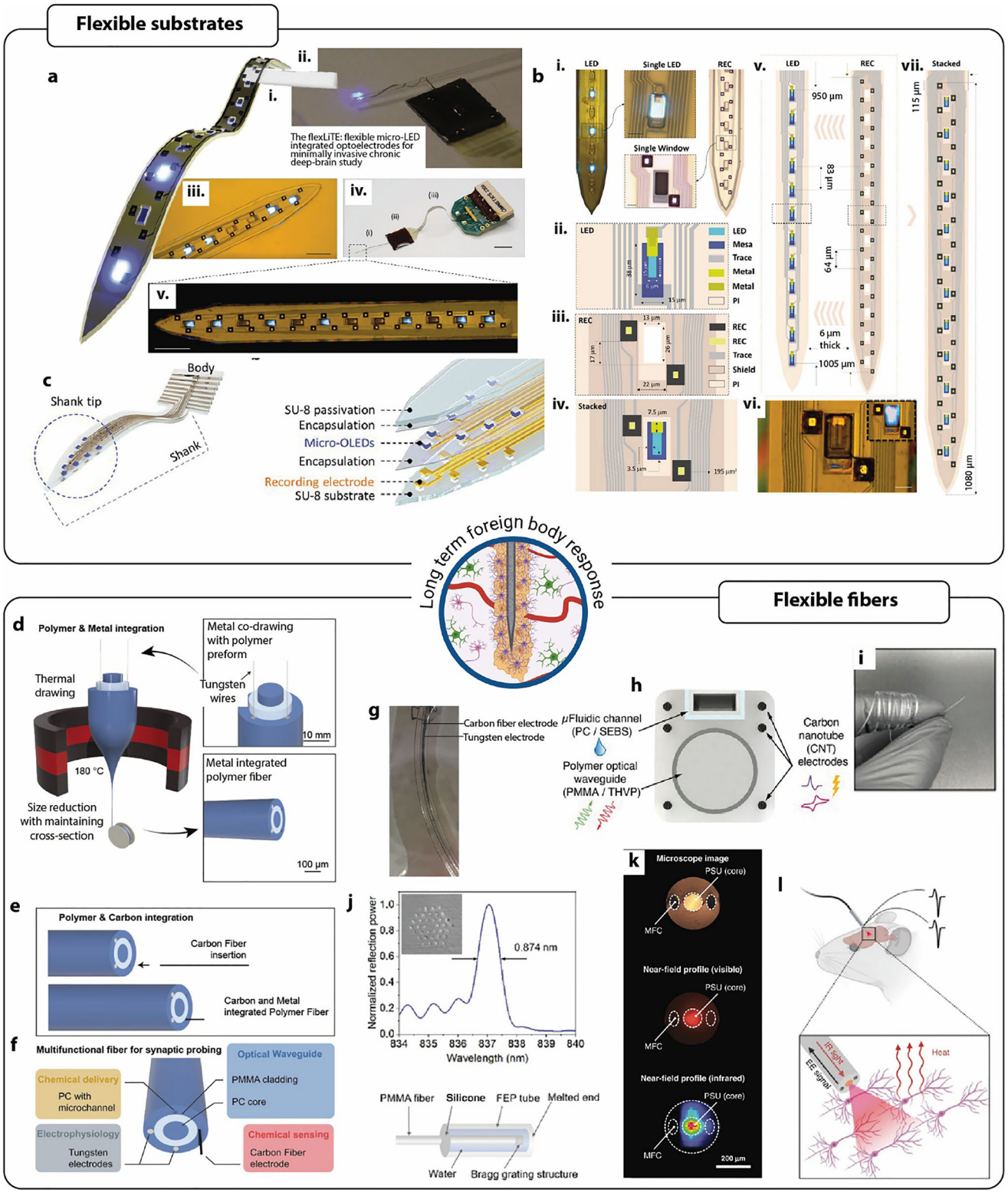

FIGURE 3 | Multifunctional neural probes with reduced FBR. (a) The flexLiTE probe. (i) Schematic image of the probe featuring 12 µLEDs and 32 recording microelectrodes. (ii) A 10-mm long shank of the flexLiTE wrapping around a 200 µm diameter optical fiber twice with µLEDs turned on. (iii) Magnified image of the front end of the probe. Scale bar: 100 µm. (iv) Bird's eye view of an assembled probe including a silicon interposer that connects the probe's frontend to a cable by ball bonding, and a flexible cable with metal traces for further connection to a headstage PCB. Scale bar: 1 mm. (v) Microscope image of the inset of (iv). Scale bar: 100 µm. (b) Modular stacking and assembly of flexLiTE optrodes and critical dimensions. (i) Microscope image of the released LED and REC probe. (ii) Schematic illustration of an LED and dimensions. (iii) Schematic illustration of an LED window and two recording electrodes and dimensions. (iv) Schematic illustration of the stack of (ii) and (iii). (v) Schematic of LED and REC probes with

monitoring of chemical and electrophysiological signals with optical and chemical stimulation in an overall diameter of 250 μm. Importantly, despite the incorporation of stiff materials (e.g. tungsten and carbon fiber electrodes) the probe retained its flexibility (Figure 3g) as its effective mechanical behavior is dominated by the surounding polymer matrix. This compliance enables the probe to better accommodate brain micromotion, reducing interfacial shear stress and thereby mitigating chronic inflammatory responses. Following the same concept, Driscoll et al. [20] realized a compact, integrated bidirectional probe—known as Polymer-based Optical-electrical-chemical neurological Interface (POLI) fiber—comprising of CNT electrodes, polymer optical waveguides and microfluidic channels (Figure 3h,i). The unique feature of this probe is its magnetic resonance imaging (MRI) compatibility, owing to the low magnetic susceptibility of the CNT electrodes. This is a highly favorable property toward the prospective clinical translation of the probe. Notably, thermally drawn POFs have been additionally equipped with the capability to measure local brain temperature. Monitoring temperature variations in the brain is of critical importance as these variations are directly linked to changes in neural activity [100]. Localized temperature variations can be also indicative of a neurological disease or a traumatic brain injury, while in the field of optogenetics, real-time monitoring of brain temperature can assist in managing light-induced thermal effects. To sense temperature variations in vivo, Sui et al. inscribed a fiber Bragg grating (FBG)—reflective microstructures featuring periodic variations in the refractive index—whose expansion or shrinkage due to a temperature change results in a change of reflected wavelength (Figure 3j), achieving sensitivity of 33pm/°C and accuracy of <0.2°C [101].

TDP-fabricated fibers have also been successfully employed in infrared neurostimulation (INS), which is gaining the attention of the neuroscience community as a viable transgene-free alternative to optogenetics [102]. INS is based on infrared light absorption from tissue and it influences neural activity via temperature-mediated processes. In this context, Meneghetti et al. [103] achieved high infrared light transmission by employing PSU and fluorinated ethylene propylene (FEP) copolymer as materials for the fiber core and cladding, respectively (Figure 3k). The thermally drawn structured POF integrated also microelectrodes for simultaneous extracellular electrophysiology (Figure 3l). This soft monolithic optoelectrical probe demonstrated the ability to deliver IR light over a wide spectral range (450–2100 nm) and stimulate neural circuitry in cortical domains with very low inflammatory response while recording high SNR electrophysiological signals.

A key challenge for flexible multifunctional neural probes is their tendency to buckle during implantation, requiring assisted insertion. This limitation is shared with single-modality flexible neural implants, allowing multifunctional probes to leverage existing implantation strategies. Such methods include the use of an external shuttle [104] or the coating of the probe with bioresorbable stiffeners such as polyethyleneglycol (PEG) [86, 105] and silk fibroin [106]. While effective in facilitating implantation, these approaches can influence the induced FBR by modifying the extent of acute tissue damage and early inflammatory signaling at the implantation site. Other implantation strategies are based on electrical and ultrasonic microactuation during insertion [107]. Here, high velocity vibrations at the insertion tip, provided by the integrated piezoelectric transducers, result in cutting of the tissue ultrasonically during penetration, leading to successful insertion with reduced trauma [108]. Beyond implantation mechanics, the surface physicochemical properties of the probe—wettability, surface roughness and charge—may further contribute to the induced FBR. The effect is indeed twofold: (i) impose a certain distribution of strain values during implantation leading to an augmented localized trauma and (ii) enhance the non-specific absorption of serum protein on the probe's surface, proven to drive the activation of microglia [109]. These can be mitigated by lubrication of the probe [110] to minimize friction during insertion and the use of antifouling coatings [111], whose role is to reduce the interaction between the body fluid and the surface of the probe by preventing protein absorption. Moreover, bioactive coatings have also been developed, aiming at delivering anti-inflammatory drugs [112] and anti-oxidants [113], at the device-tissue interface.

Overall, the progress of the past few years has defined a clear path toward minimizing the FBR associated with implantable optoelectrical neural probes. The translation of μLED and micro-OLED-based optrodes on flexible substrates will offer, indeed, a more seamless mechanical matching with the brain tissue, permitting their use in chronic settings. Given their unique characteristics, including superior flexibility, low thermal footprint and ease of integration, micro-OLEDs can potentially replace μLEDs as the dominant light source in the development of next-generation optoelectrical devices for neural interfacing. At the

design parameters. The REC probe is stacked on top of the LED probe. (vi) Microscope image of the stacked probe showing a LED aligned inside the window of the REC probe. Scale bar: 10 μm. (vii) Schematic of the stacked probe with design parameters. Reproduced with permission [92]. Copyright 2024, Ko et al., bioRxiv. (c) Schematic illustration of the flexible OLED probe and cross-sectional view of the total device. Reproduced under terms of the CC-BY-NC-ND 4.0 International license [33]. Copyright 2025, Wiley-VCH GmbH. (d,e) Schematic illustration of the fabrication of the multifunctional fiber using the TDP. (f) Schematic illustration of the multifunctional fiber and its components. (g) Image of the multifunctional fiber under bending condition. Reproduced under terms of the CC-BY-NC-ND 4.0 International license [99]. Copyright 2024, The Authors, American Chemical Society. (h) Schematic illustration of the cross-section of the POLI fiber, highlighting its recording and stimulation capabilities. (i) Photograph highlighting the flexibility and microscopic size of the fiber. Reproduced under terms of the CC-BY license [20]. Copyright 2024, The Authors, Wiley-VCH GmbH. (j) Top: Normalized reflectance spectrum of the FBG. The inset shows the optical image of the cross section of the fabricated fibers. Bottom: Detailed material and structure overview of the assembled brain temperature sensor. Reproduced with permission [101]. Copyright 2023, Optica Publishing Group. (k) From top to bottom: Microscope image of the structure of the fabricated optical fiber and near-field profiles of the output light at both visible and IR wavelengths. (l) Conceptual figure illustrating the simultaneous performance of IR neurostimulation and electrophysiology using the fabricated fiber. Reproduced under terms of the CC-BY license [103]. Copyright 2023, The Authors, Springer Nature.

same time, thermally drawn POFs, which are already the leading candidates toward the realization of flexible, multifunctional neural probes, will continue to evolve thanks to the development of novel polymer preforms that will expand their functionalities and applications. However, flexible optoelectrical neural probes will only reach their full potential when accompanied by continued innovation in implantation strategies, which currently represent the primary bottleneck for their further development. Future implantation strategies will likely focus more on the employment of smart materials with adaptable stiffness, such as shape memory polymers [114] and stimuli-responsive materials [115]. Such materials will provide probes with temporary rigidity for the insertion, which will then be reversed in vivo in order to comply with the mechanical properties of the brain tissue. The same materials will be able to reduce protein adsorption and dynamically modulate the local microenvironment of the implant in closed-loop, thus ensuring its long-term biocompatibility and performance.

2.3 | Neurochemical Sensing

Neuronal function is the result of a complex electrochemical signaling process, where neurotransmitters, ions, metabolites, cytokines and ROS collectively modulate brain physiology, mediating both normal and pathological processes [25]. Among these, neurotransmitters serve as the principal chemical messengers of the central nervous system, orchestrating the function and homeostasis of both central and systemic physiological processes [116]. Dysregulation of neurotransmitter dynamics has been strongly implicated in several major neurodegenerative and neuropsychiatric disorders, including PD and AD [26]. Ions such as potassium (K^+) and calcium (Ca^{2+}) bridge chemical and electrical signaling, governing membrane excitability and synaptic transmission [117], while metabolic markers including glucose, lactate and pH reflect the energetic state of neurons and glia, contextualizing neurotransmission within metabolic activity [118, 119]. Finally, cytokines act as neuromodulators, linking the immune and nervous systems and integrating inflammatory, metabolic and synaptic signals. Although their effects are slower and more diffused than fast synaptic neurotransmission, cytokine signaling is necessary to maintain homeostatic behavior [120].

Consequently, there is growing recognition that fully understanding of neuronal function requires sensing platforms capable of simultaneously capturing electrical and chemical dynamics. While traditional electrophysiological methods provide high-resolution measurements of neuronal activity, they offer limited insight into the accompanying neurochemical changes, which are critical for interpreting complex physiological and pathological processes. Similarly, single-modality chemical sensors, though capable of detecting specific molecular events, cannot capture the temporal and spatial patterns of neuronal signaling on their own. Importantly, only spatially co-registered optoelectrical and neurochemical interfaces ensure that electrical and chemical readouts originate from the same cellular or microcircuit environment. This co-localization is methodologically critical for establishing direct spatiotemporal correlations and enabling explicit mechanistic interpretation, which cannot be reliably achieved when using spatially separated devices. Such integrated systems therefore enable: (i) better contextualization of molecular signaling alongside electrical activity detected at much higher spatio-temporal resolution, and (ii) causal investigation of neurochemical release by exploiting simultaneous and co-localized cell-specific optical neural stimulation. By moving beyond conventional correlative approaches, these platforms allow the exploration of neural dynamics from new perspectives. Beyond fundamental research, such integrated systems may hold significant promise for translational applications, particularly by enabling patient-informed therapeutic strategies and interventions for neurological and neuropsychiatric disorders such as depression [121].

The potential for integration is revolving around three main technologies: electrochemical sensing, genetically encoded fluorescent indicators (GEFIs) of neurochemical concentrations, and surface enhanced Raman spectroscopy (SERS). Here, we choose to focus on neurotransmitter sensing. Neurotransmitters—including DA, serotonin, GABA, glutamite and histamine—are the most frequently targeted analytes by the scientific community working on implantable neural interfaces, owing to their high clinical relevance [122, 123].

Successful sensing of neurotransmitters requires high sensitivity as the physiological concentration of neurotransmitters in the brain is extremely low ranging from nanomolar (nM) to micromolar (μM) levels [124]. Electrochemical sensors based on implantable microelectrodes provide a promising platform for real-time monitoring of these neurochemical signals. These sensors operate by measuring current changes resulting from redox reactions of neurotransmitters or their metabolites at the electrode surface. While this method offers excellent sensitivity, it suffers from limited specificity, as many biomolecules possess overlapping redox potentials that can generate indistinguishable electrochemical signatures. To address this limitation, electrode surfaces can be functionalized with molecular recognition elements such as natural enzymes, which selectively catalyze specific target molecules [25]. However, the diversity of available enzymes is inherently restricted. Recent advances in nanomaterials have enabled the development of biomimetic enzyme structures, expanding the range of detectable analytes [125]. Additionally, aptamer-modified electrodes have been employed for their high binding specificity to particular neurotransmitters [126]. Nonetheless, both enzymatic and aptamer-based recognition strategies often involve binding kinetics that limit the temporal resolution, making it challenging to track fast neurochemical dynamics in real time.

One of the main challenges of integrating this sensing capability in optoelectrical neural interfaces is the demand for downscaling to fit the probe's size. This leads to a reduced active surface area of the sensor and consequently to high electrochemical impedance, implying a reduced SNR that impacts the detection limit [127]. An effective approach to decrease the impedance of an electrode while maintaining a reasonable surface (hundreds of μm^2) consists in introducing 3D structuring or roughness to increase the electrode's effective surface area on the same footprint [128]. This approach has been followed for multifunctional neural interfaces by exploiting carbon-based nanostructured materials such as CF [129], CNT and graphene [130]. Stuart et al. managed to combine optogenetic stimulation with electrochemical recording of transient DA dynamics in a miniaturized probe featuring a μLED and

a CNT-based sensor (Figure 4a) exhibiting a sensitivity among the highest reported in the literature (1264.1 nA μM^{-1} cm^{-2}) [131]. In general, carbon-based microfiber electrodes exhibit superior electrochemical stability compared to conventional platinum microelectrodes; a property that reinforces their long-term performance. In a recent study, Castagnola et al. demonstrated a fully customizable batch fabrication of ultra-miniaturized 5-shank/15-channel glassy carbon fiber-like (GCF) MEA probes (Figure 4b) able to perform DA and serotonin detection combined with single-unit electrical recordings (Figure 4c) [132]. One of the interesting features of those probes is that despite their flexibility, they do not require an assisted insertion by virtue of their stiff backbone, and thus have a minimal footprint.

Still aiming at reduced impedance, organic conductive polymers are a promising alternative to nano-structuring. Their highly porous morphology naturally increases the electroactive area and facilitates electronic and ionic charge transport. Among the conductive polymers available, poly(3,4-ethylenedioxythiophene) polystyrene sulfonate (PEDOT:PSS) is the most widely adopted by virtue of its excellent electrical conductivity, ease of electrodeposition on micro-structured surfaces, and ability to conformally coat complex geometries along with its high biocompatibility and stability in aqueous media [133]. In particular, a 100 nm thick coating of PEDOT:PSS can result in a 100-fold drop in the impedance of a gold electrode [134]. An alternative material that has recently gained interest is PEDOT:Nafion. Carli et al. demonstrated that flexible neural microelectrodes electrodeposited with PEDOT:Nafion exhibit a charge injection limit two times larger than that observed for their PEDOT:PSS counterparts [135]. However, despite these benefits, both PEDOT:PSS and PEDOT:Nafion have so far been applied primarily to enhance electrical recording and stimulation in MEAs, and — to the best of our knowledge — have not yet been integrated for neurotransmitter sensing in optoelectrical platforms based on μLEDs, waveguide arrays, or optical fibers.

One of the main concerns related to the use of electrochemical sensing electrodes is their long-term stability in vivo. Section 2.2 highlights how progressive FBR disrupts the neurochemical microenvironment around the probe, causing accumulation of ROS and nonspecific adsorption of proteins on its surface, which can hinder the diffusion of molecules of interest in the sensing area. As a consequence, electrode biofouling and cellular encapsulation lead to a gradual loss of sensitivity, increased noise, and shifts in baseline currents, all of which compromise detection limits and invalidate initial calibrations over time. In particular, in fast-scan cycle voltammetry measurements, biofouling appears as a drift in the peak oxidation potential of the baseline signal, progressively increasing over days to weeks, thereby reducing the responsiveness and specificity of the electrode to neurotransmitters [136]. One mitigation approach includes preconditioning pulses and optimized scan waveforms, which remove adsorbed species and reduce surface etching. Researchers have also been focused in developing implantable electrochemical sensors with anti-inflammatory capacity. That consists in coating the electroactive area of the sensing probes with antioxidants (either natural or synthetic) [113].

Another emerging technology for neurochemical sensing in neural interfaces is the organic electrochemical transistor (OECT). OECTs differ fundamentally from traditional electrode-based sensors in the fact that they combine amplification and sensing functions within a single miniaturized device. These transistors operate by transducing ionic changes in the surrounding biological environment—such as neurotransmitter concentrations—into modulations of electronic current through an organic semiconductor channel. This intrinsic amplification enables high sensitivity at extremely low analyte concentrations, down to the nanomolar range, even with minimal sensor surface area [137]. OECTs also exhibit low operating voltage (< 1 V), excellent temporal resolution (on the order of milliseconds), and mechanical flexibility, making them particularly suitable for chronic, tissue-compliant implants [138]. OECTs best performances are obtained when recording low-frequency signals and offer great advantages in terms of initial noise. Indeed, their SNR is five to ten times higher than passive metal electrodes, ranging in the order of tens of dB and strictly depending on the application [139]. As a drawback, OECTs are more prone to ionic drift because of ion redistribution as short-term effect, partial ion trapping as mid-term effect and overoxidation in the long time range, affecting SNR over timescales of days and weeks [140]. Approaches involving electrochemical modification to the floating gate [141], cross-linked PEDOT:PSS and other conducting polymers can reduce ionic drift over time [142], but strictly depend on the application since some of them lack biocompatibility.

Recent studies have demonstrated the feasibility of integrating OECTs onto implantable neural probes for in vivo detection of DA and catecholamines (Figure 4d), with simultaneous readout from multiple transistor sites arranged in array formats [35, 143]. Importantly, these platforms are inherently compatible with optical neural interfaces, as their design allows the sensor and the optical path to be spatially decoupled. In principle, OECT arrays can be integrated with waveguides, μLEDs, or tapered fibers, enabling multimodal probes that can sense neurotransmitter dynamics while simultaneously delivering or detecting light. Despite their integration into optical neural interfaces being still at an early stage, the low power consumption, on-device amplification, and compatibility with soft substrates position OECTs as promising candidates for future multifunctional opto-electro-chemical neural interfaces.

An alternative to electrode- and OECT-based sensing is offered by GEFIs. They provide cell-type-specific readouts of neurochemical dynamics using optical signals and can be collected with either SPADs or fiber based devices described at the end of Section 2.1. These sensors are designed by fusing fluorescent proteins with receptor domains that undergo conformational changes upon binding to specific neurotransmitters, resulting in detectable changes in fluorescence intensity or wavelength. One of the most prominent examples is dLight1; a DA-sensitive fluorescent reporter developed by fusing a circularly permuted green fluorescent protein (GFP) to the DA receptor D1 [5]. dLight1 enables the detection of fast, transient DA signals in vivo with high temporal and spatial resolution (Figure 4e) and has since been expanded into a palette of color variants for multiplexed sensing [8]. Building on this concept, several research teams have created genetically encoded sensors for other neurotransmitters, including: $GRAB_{NE}$ for norepinephrine [144], $GRAB_{5\text{-}HT}$ for serotonin [144], iAchSnFr for acetylcholine [144], and sensors for GABA, glutamate, adenosine, and histamine [145]. These indicators are

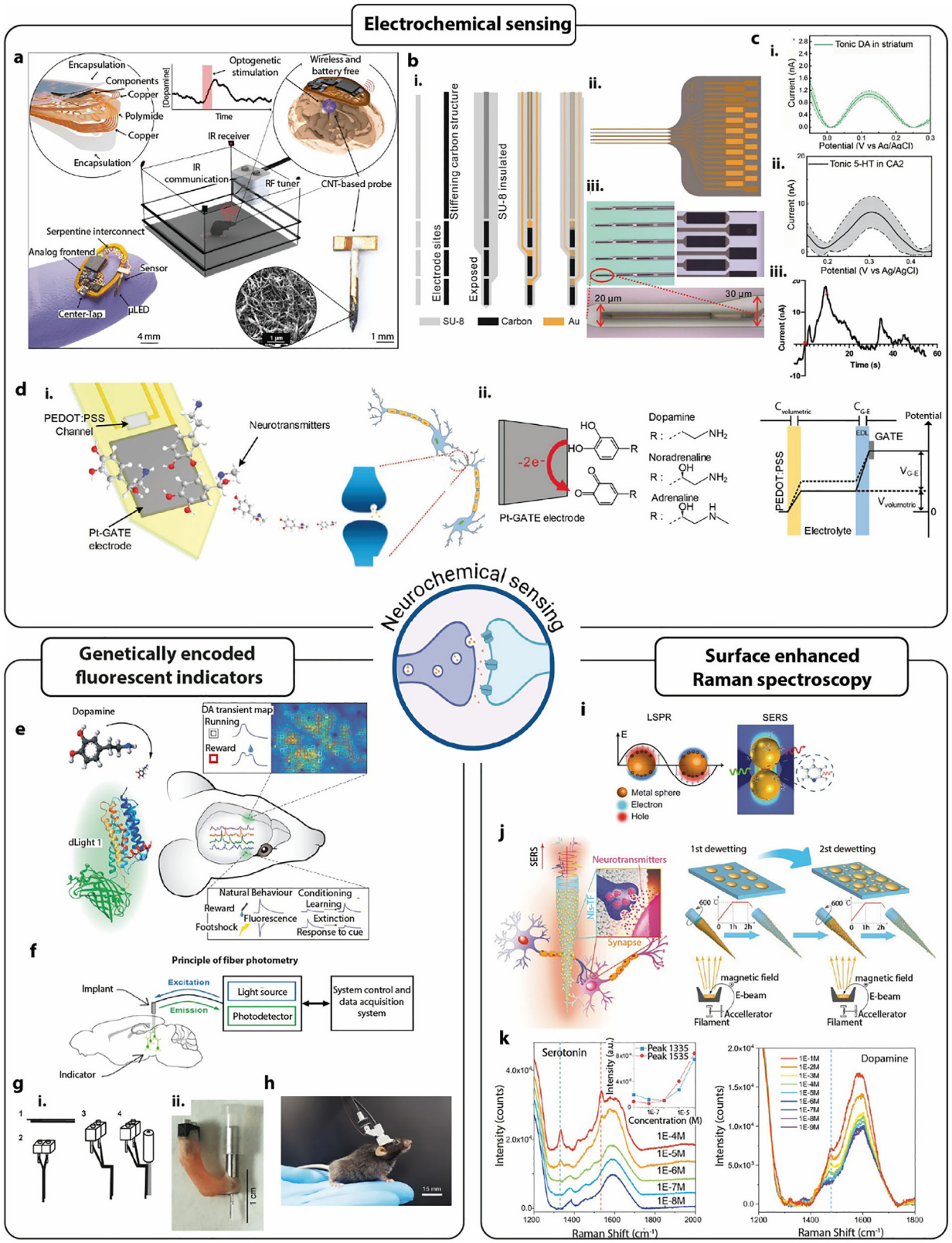

FIGURE 4 | Technologies for neurochemical sensing in vivo. (a) Conceptual figure illustrating the operational principle of the subdermally implantable, wireless, and battery-free device capable of real-time, multimodal optogenetic stimulation and electrochemical recording of transient DA dynamics in the brain. Reproduced with permission [131]. Copyright 2023, American Chemical Society. (b) Design and fabrication of GCF MEAs. (i) The fabrication process of the GCF. SU-8 is spin-coated and patterned on a wafer, followed by pyrolysis to produce carbon electrode sites and the stiffening structure. SU-8 is spin-coated and patterned to insulate the stiffening structure but exposing the electrode sites. Metal is patterned using lift-off procedures. A top layer of SU-8 is patterned to insulate the metal patterns. (ii) The layout of the GCF. (iii) Optical microscopy images of the GCF. (c) In vivo detection of dopamine and serotonin with GCF MEAs. (i) Square wave voltammetry detection of tonic DA. (ii) Square wave voltammetry

typically used in combination with fiber photometry (Figure 4f), where an optical fiber implanted into the brain both excites the sensor and collects the emitted fluorescence [146]. This approach has been widely adopted due to its simplicity and compatibility with freely moving animals [147]. Integration into optoelectrical neural interfaces is naturally compatible, especially in fiber-based systems, where the same or adjacent optical path can be used for both fluorescence readout and optogenetic stimulation [148]. Further boosting multifunctionality, Patel et al. [149] have demonstrated a hybrid implant that couples a bipolar electrode with an optical fiber cannula (Figure 4g), enabling simultaneous recording of sub-second field potentials alongside cell-type-specific fiber photometry. These detection methods can be also coupled with CNT for cyclic voltammetry for electrochemical detection of neurotransmitters and optogenetics, by exploiting the thermally drawn ultra-flexible polymeric fiber technology discussed in Section 2.2 [150]. A key advantage of GEFIs lies in their molecular nature, which allows seamless compatibility with fluorescence-based endoscopic imaging at subcellular resolution. This has enabled the implementation of single-cell resolution optogenetics and neurotransmitter imaging using fiber-coupled or head-mounted miniaturized microscopes (Figure 4h) [151, 152]. Looking forward, a major goal is the development of fully integrated platforms that combine high-resolution optical imaging with electrophysiological recording, enabling simultaneous readout of cellular activity and neuromodulator dynamics. This would offer a powerful approach to dissect causal relationships between chemical signaling and circuit-level electrical activity, particularly in behaving animal models of disease and cognition.

Since genetically encoded indicators rely on genetic modifications of the organism under study, their application is limited to lab animal models. In this context, label-free technologies that can be exploited in vivo in wild-type models have emerged as a promising alternative with high translational potential for future human applications. As an example, high sensitivity in vivo sensing of neurotransmitters and neuromodulator dynamics has also been achieved by Kong and colleagues thanks to the development of a technology based on engineered cells on fiber optic probes (FOPECs) [153]. This plug and play approach can overcome the need for viral injection or genetic expression of optogenetically active molecules in the animal of interest by integrating cells expressing the fluorescent neurotransmitter sensor directly onto the tip of an optic fiber. Despite the fact that the response of FOPECs is diffusion limited and depends on the physical properties of the hydrogel used as embedding layer, they display high specificity, low detection limit, and wide dynamic range.

Another recent and label-free strategy for neurochemical sensing leverages SERS, which enables ultrasensitive molecular fingerprinting of neurotransmitters based on their vibrational spectra. SERS relies on the enhancement of Raman scattering signals that occurs when analytes are in close proximity to nanostructured metallic surfaces—typically gold or silver nanostructures—that support localized surface plasmon resonances (Figure 4i) [154]. Despite not yet been tested in vivo, Zheng et al. [36, 155] demonstrated the use of gold nanoislands integrated on tapered fibers with a wide optically-active surface to detect DA and serotonin through SERS with sub-10 nm plasmonic gaps, enabling high spectral resolution and detection at μM concentrations (Figure 4j,k). This architecture benefits from the intrinsic compatibility of optical fibers with deep brain implantation and minimal tissue damage, while also allowing the same platform to be used for optical stimulation or photometry. However, integrating SERS into multifunctional optoelectrical neural interfaces is still in its infancy, due to current limitations related to stable nanostructure fabrication, low background signals, and real-time spectral deconvolution. Indeed, while the nanoparticle nucleation approach presented above represents a highly precise nanofabrication technique, it is incompatible with standard microfabrication and patterning processes used for TFs, thereby limiting its broader applicability. Nevertheless, SERS has demonstrated the detection of neurotransmitters with sensitivity reaching attomolar concentrations [156]. Therefore, as SERS-compatible fiber designs continue to evolve, this approach offers a promising route toward label-free, multiplexed neurochemical

detection of tonic 5-HT (serotonin). (iii) Fast scan cyclic voltammetry detection of stimulated DA. Reproduced under terms of the CC-BY license [132]. Copyright 2024, The Authors, Wiley-VCH GmbH. (d) The OECT-array implantable probe. (i) Schematic illustration of the use of the OECT for monitoring neurotransmitter release. (ii) Schematic illustration of CA-NT's electro-oxidation reaction on the surface of the Pt-GATE electrode and diagram showing the working principle of the OECT device. Reproduced under terms of the CC-BY license [35]. Copyright 2020, Xie et al. (e) Conceptual figure illustrating high resolution imaging of dopamine in vivo using the dLight1. In particular, dynamic learning-induced dopamine changes in the nucleus accumbens (bottom) and task-specific dopamine transients in the cortex (top). Reproduced with permission [5]. Copyright 2018, The American Association for the Advancement of Science. (f) Schematic illustration of the principle of fiber photometry. Reproduced under terms of the CC-BY license [147]. Copyright 2023, The Authors, SPIE. (g) The hybrid implant featuring a bipolar electrode and an optical fiber cannula. (i) Fabrication process steps. (ii) Photograph of the assembled implant. Reproduced under terms of the CC-BY license [149]. Copyright 2020, Patel, McAlinden, Mathieson, and Sakata. (h) Photograph of a mouse wearing a fast, high-resolution, miniaturized two-photon microscope headpiece. Reproduced with permission [152]. Copyright 2021, The Authors, Springer Nature. (i) Left: Schematic illustration of the localized surface plasmon resonant effect (LSPR): Metal conductive electrons are excited into collective oscillations generating an electromagnetic (EM) field highly localized in the metal-dielectric interface when irradiated with light. Right: Nanoparticle-molecule interaction leading to the mutual excitation of the Raman polarizability (red thin arrow) from the local EM field (green arrow) and generating the enhanced Raman signal of molecule (red thick arrow). Reproduced under terms of the CC-BY license [154]. Copyright 2020, Royal Society of Chemistry. (j) Schematic illustration of gold nanoislands-decorated TFs for neurotransmitters' SERS signal detection and their fabrication procedure. (k) Left: Detection of serotonin aqueous solution with concentrations varying from 10^{-8} to 10^{-4} M. The inset shows the concentration dependence of the area under 1335 cm^{-1} (blue points) and 1535 cm^{-1}(red points) after locally subtracting the background. Right: Detection of dopamine aqueous solution with concentrations varying from 10^{-9} to 10^{-1} M. The blue vertical dashed line indicates the dopamine peak at 1476 cm^{-1}. Reproduced under terms of the CC-BY-NC 4.0 license [36]. Copyright 2023, Wiley-VCH GmbH.

TABLE 2 | Summary of the multimodal devices featured in the Review.

Device	*Mechanical behavior*		*Modality*			*Application*		
	Rigid	**Flexible**	**Optical**	**Electrical**	**Chemical**	**Target brain region**	**Acute**	**Chronic**
Wireless battery-free implant [131]		X	X		X	mouse nucleus accumbens	X	X
Fibertrobe [32]	X		X	X		mouse striatum & cortex	X	
TDP-fiber probe [99]		X	X	X	X	mouse striatum	X	X
FlexLiTE [92]		X	X	X		mouse hippocampus	X	X
HectoSTAR probe [30]	X		X	X		mouse cortex & hippocampus	X	
miniSTAR probe [53]	X		X	X		mouse hippocampus	X	
POLI fiber probe [20]		X	X	X	X	mouse ventral tegmental area & nucleus accumbens	X	X
Micro-OLED probe [33]		X	X	X		in vivo work not reported		
Neuropixels Opto [31]	X		X	X		mouse cortex & striatum	X	
Glassy Carbon-like MEAs [132]		X		X	X	mouse striatum	X	X
DuoLite [58]	X		X	X		mouse cortex	X	
INS probe [103]		X	X	X		rat cortex & hippocampus	X	X
Hybrid probe [149]	X			X	X	mouse mesopontine tegmentum		X
Dual-color nanophotonic probe [60]	X		X	X		mouse cortex	X	

sensing in vivo, particularly when combined with other optical modalities.

Multifunctional neurochemical sensing has now become one of the key research focus for the neurotechnology community, aiming at complementing electrical recording and optical stimulation and allowing for a more comprehensive picture of neural signal. This has been enabled by advances in electrochemical sensing using implantable microelectrode arrays, the introduction of large-gate OECTs, the expansion of the GEFI palette and the introduction of label-free optical detection using optical fibers. OECT-based neurochemical sensing is receiving increasing attention mainly due to its intrinsic amplification capabilities and compatibility with soft and flexible substrates, which make it particularly well-suited for compact and chronically implantable neural probes. In parallel, TFs are rapidly emerging as a highly versatile and minimally invasive platform for multimodal sensing and actuation of neural activity. Their conical geometry not only facilitates efficient light delivery for optogenetic stimulation and simultaneous fluorescence collection, but also provides an adaptable interface for integrating advanced photonic sensing modalities. Notably, coupling TFs with SERS-active nanostructures—through either evanescent or propagative modes—may allow in the near future for in vivo label-free, multiplexed neurochemical sensing [157]. This convergence of optical stimulation, functional imaging and label-free chemical fingerprinting within a single probe, places optical waveguides at the forefront of next-generation multifunctional neural interfaces. Looking forward, integrating multiple OECTs on fiber optics could transform them from passive multimodal probes to active neuromorphic devices allowing for on-probe computation, thus minimizing data transfer bottlenecks and enabling real-time adaptive modulation of neural circuits.

3 | Conclusions and Future Perspectives

The convergence of optical stimulation, extracellular recording, and neurochemical sensing within a single implantable neural interface represents a transformative objective for systems neuroscience, neurotechnology, and neuroengineering. Recent advances in microfabrication, flexible materials, and nanophotonic integration have enabled the development of increasingly sophisticated multifunctional devices. To date, however, most implementations integrate mostly two modalities of interaction with neural tissue, while devices combining three or more functionalities remain relatively scarce. This is also reflected in Table 2, which provides a summary of the main multimodal devices discussed in the review. In particular, out of the 14 devices considered, only two exhibit all three modalities (optical, electrical and chemical). Interestingly, both devices are based on thermally drawn POFs highlighting the clear advantage of this technology in terms of multimodal integration.

Despite significant advances over the past decade, front-end technologies for multifunctional implantable neural systems continue to face several critical challenges. Integration density remains limited by fundamental trade-offs among device footprint, and thermal load, while long-term performance is compromised by foreign body responses and mechanical mismatch with brain tissue. In addition, although highly promising, the incorporation of neurochemical sensing is still largely confined to proof-of-concept demonstrations. Looking ahead, further progress will require scalable fabrication approaches that preserve both flexibility and functionality, as well as strategies to actively modulate host tissue responses, for example through bioactive or resorbable coatings. Moreover, effective cross-compatibility among sensing and actuation modalities—optical, electrical, chemical, and thermal—will be essential to achieve truly multimodal, high-resolution brain interfaces, together with closed-loop platforms enabling real-time, multisite stimulation and sensing.

Beyond the implantable portion of the device, it is important to note that the field is in parallel actively working on developing back-end solutions associated with power consumption, wireless powering, data links and packaging aspects [28]. Moreover, multimodal capabilities generate the need for defining more effective algorithms and analytical pipelines specifically tailored to multimodal data handling. Conventional acquisition systems and off-line post hoc processing are indeed being proven insufficient for real-time multimodal experiments [15]. One of the core challenges of the scientific community, in this context, is the spatio-temporal mismatch across the heterogeneous signals acquired, including optical, chemical and electrophysiological readouts. Indeed, implantable optoelectrical devices rely often on the analysis of brain volumes that range from few micrometers to millimeters and collect signals related to events that span from milliseconds to seconds [90]. In this context, the alignment of signals occurring at such different spatial and temporal scales is fundamental for a correct representation and interpretation of neural activity, from single cell-level to cell population behavior and brain areas connectivity. Other critical challenges in multimodal data handling include addressing motion artifact removal across modalities and the cross-scale feature extraction capable of linking single-cell to network and behavioral dynamics. In this context, a new generation of tools is being developed, where classical methods, including spike sorting, dimensionality reduction, and functional connectivity analysis, are being supported by a wide set of emerging machine learning (ML)- and artificial intelligence (AI)-driven approaches [16]. ML tools play a fundamental role in managing high-dimensional data, handling noise and inter-subject variability as well as capturing nonlinear and higher-order relationships [158]. ML-based classification approaches can reveal subtle, condition-specific patterns across a large pool of data. For instance, a model trained on electrophysiological recordings could distinguish experimental brain metastasis subtypes based on their effects on neural circuits [159], while deep learning models can be trained to distinguish and remove motion artifacts from acquired signals [73]. Moreover, the ability of ML-driven approaches to integrate multiple data streams in real-time together with advances in next generation implantable optoelectonics, might be the answer to the long standing quest for closed-loop control through adaptive real-time modulation of neural signals [75].

Taken together, addressing these challenges will not only deepen our understanding of neural dynamics, but also open new avenues for precision neuromodulation in clinical and neuroprosthetic applications.

Acknowledgments

Open access publishing facilitated by Istituto Italiano di Tecnologia, as part of the Wiley - CRUI-CARE agreement.

Funding

M.D.V. and F.P. jointly supervised and are co-last authors in this work. S.A., M.D.V. and F.P. acknowledge funding by the European Union (ERC, MINING, 101125498). Views and opinions expressed are however those of the author(s) only and do not necessarily reflect those of the European Union or the European Research Council. Neither the European Union nor the granting authority can be held responsible for them. B.S., M.D.V., and F.P. acknowledge funding from the Project "RAISE (Robotics and AI for Socio-economic Empowerment)" code ECS00000035 funded by European Union – NextGenerationEU PNRR MUR – M4C2 – Investimento 1.5 – Avviso "Ecosistemi dell'Innovazione" CUP J33C22001220001. S.A., B.S., M.D.V., and F.P. acknowledge that this project has received funding from the European Union's Horizon 2020 Research and Innovation Program under Grant Agreement No. 101016787. S.A., B.S., M.D.V. and F.P. acknowledge financial support under the National Recovery and Resilience Plan (NRRP), Mission 4 "Education and Research" – Component 2 "From Research to Business" – Investment 1.3, funded by the European Union – NextGenerationEU, within the framework of the cascade funding call of Spoke 3 – Extended Partnerships among Universities, Research Centers, and Enterprises for Research Project Funding, "Mnesys" (PE00000006). This work is part of the project "Correlating multifunctional signals in 3D printed neurochips for next generation studies on neural degeneration, via spectroscopy and electrophysiological recordings" (acronym: COMBO) – CUP: E63C22002170007. A.B. acknowledges funding from the European Union's Horizon 2020 research and innovation programme under the Marie Sklodowska-Curie grant agreement (#101106602). M.D.V. acknowledges funding from the Novo Nordisk Foundation (project SUPER, grant n.NNF23OC0079433).

Conflicts of Interest

M.D.V. and F.P. are founders and hold private equity in OptogeniX, a company that develops, produces, and sells technologies to deliver light into the brain.

Data Availability Statement

The authors have nothing to report.

References

1. L. Guo, "Perspectives on Electrical Neural Recording: A Revisit to the Fundamental Concepts," *Journal of Neural Engineering* 17, no. 1 (2020): 013001, https://doi.org/10.1088/1741-2552/ab702f.

2. A. H. Marblestone, B. M. Zamft, Y. G. Maguire, et al., "Physical Principles for Scalable Neural Recording," *Frontiers in Computational Neuroscience* 7 (2013): 137, https://doi.org/10.3389/fncom.2013.00137.

3. L. Fenno, O. Yizhar, and K. Deisseroth, "The Development and Application of Optogenetics," *Annual Review of Neuroscience* 34 (2011): 389–412, https://doi.org/10.1146/annurev-neuro-061010-113817.

4. T.-W. Chen, T. J. Wardill, Y. Sun, et al., "Ultrasensitive Fluorescent Proteins for Imaging Neuronal Activity," *Nature* 499, no. 7458 (2013): 295–300, https://doi.org/10.1038/nature12354.

5. T. Patriarchi, J. R. Cho, K. Merten, et al., "Ultrafast Neuronal Imaging of Dopamine Dynamics With Designed Genetically Encoded Sensors," *Science* 360, no. 6396 (2018): aat4422.

6. H. Mutoh, W. Akemann, and T. Knopfel, "Genetically Engineered Fluorescent Voltage Reporters," *ACS Chemical Neuroscience* 3, no. 8 (2012): 585–592, https://doi.org/10.1021/cn300041b.

7. V. Emiliani, A. E. Cohen, K. Deisseroth, and M. Häusser, "All-Optical Interrogation of Neural Circuits," *The Journal of Neuroscience* 35, no. 41 (2015): 13917–13926, https://doi.org/10.1523/JNEUROSCI.2916-15.2015.

8. T. Patriarchi, A. Mohebi, J. Sun, et al., "An Expanded Palette of Dopamine Sensors for Multiplex Imaging In Vivo," *Nature Methods* 17, no. 11 (2020): 1147–1155, https://doi.org/10.1038/s41592-020-0936-3.

9. S. F. El-Mashtoly and K. Gerwert, "Diagnostics and Therapy Assessment Using Label-Free Raman Imaging," *Analytical Chemistry* 94, no. 1 (2022): 120–142, https://doi.org/10.1021/acs.analchem.1c04483.

10. G. N. Angotzi, F. Boi, A. Lecomte, et al., "SiNAPS: An Implantable Active Pixel Sensor CMOS-probe for Simultaneous Large-Scale Neural Recordings," *Biosensors and Bioelectronics* 126 (2019): 355–364, https://doi.org/10.1016/j.bios.2018.10.032.

11. Y. Liu, H. Jia, H. Sun, et al., "A High-Density 1,024-channel Probe for Brain-Wide Recordings in Non-Human Primates," *Nature Neuroscience* 27 (2024): 1620–1631, https://doi.org/10.1038/s41593-024-01692-6.

12. S. M. Xu, M. Momin, S. Ahmed, et al., "Illuminating the Brain: Advances and Perspectives in Optoelectronics for Neural Activity Monitoring and Modulation," *Advanced Materials* 35, no. 42 (2023): 2303267.

13. L. Li, B. Zhang, W. Zhao, et al., "Multimodal Technologies for Closed-Loop Neural Modulation and Sensing," *Advanced Healthcare Materials* 13, no. 24 (2024): 2303289, https://doi.org/10.1002/adhm.202303289.

14. A. Arkhipov, N. da Costa, S. de Vries, et al., "Integrating Multimodal Data to Understand Cortical Circuit Architecture and Function," *Nature Neuroscience* 28, no. 4 (2025): 717–730, https://doi.org/10.1038/s41593-025-01904-7.

15. M. Ramezani, Y. Ren, E. Cubukcu, and D. Kuzum, "Innovating Beyond Electrophysiology Through Multimodal Neural Interfaces," *Nature Reviews Electrical Engineering* 2, no. 1 (2025): 42–57, https://doi.org/10.1038/s44287-024-00121-x.

16. S. Wang, S. Gordon, C. French, R. R. Unnithan, and D. Sun, "From Microelectrode Arrays to All-optical and Multimodal Neural Interfaces: Emerging Platforms for Spatiotemporal Interrogation of in Vitro Neural Circuits," *Frontiers in Synaptic Neuroscience* 17 (2025): 1732955.

17. S. Murugappan, S. A. M. Tofail, N. D. Thorat, and R. Spectroscopy, "Raman Spectroscopy: A Tool for Molecular Fingerprinting of Brain Cancer," *ACS Omega* 8, no. 31 (2023): 27845–27861, https://doi.org/10.1021/acsomega.3c01848.

18. J. Zhang, Y. Zhang, J. Wang, Y. Xia, J. Zhang, and L. Chen, "Recent Advances in Alzheimer's Disease: Mechanisms, Clinical Trials and New Drug Development Strategies," *Signal Transduction and Targeted Therapy* 9, no. 1 (2024): 211, https://doi.org/10.1038/s41392-024-01911-3.

19. J. S. Bogers, B. R. Bloem, and J. M. Den Heijer, "The Etiology of Parkinson's Disease: New Perspectives From Gene-Environment Interactions," *Journal of Parkinson's Disease* 13, no. 8 (2023): 1281–1288, https://doi.org/10.3233/JPD-230250.

20. N. Driscoll, M.-J. Antonini, T. M. Cannon, et al., "Multifunctional Neural Probes Enable Bidirectional Electrical, Optical, and Chemical Recording and Stimulation in Vivo," *Advanced Materials* 37 (2024): 2408154.

21. H. Tian, K. Xu, L. Zou, and Y. Fang, "Multimodal Neural Probes for Combined Optogenetics and Electrophysiology," *Iscience* 25, no. 1 (2022): 103612, https://doi.org/10.1016/j.isci.2021.103612.

22. G. Hong and C. M. Lieber, "Author Correction: Novel Electrode Technologies for Neural Recordings," *Nature Reviews Neuroscience* 20, no. 6 (2019): 376, https://doi.org/10.1038/s41583-019-0169-6.

23. A. Perna, G. N. Angotzi, L. Berdondini, and J. F. Ribeiro, "Advancing the Interfacing Performances of Chronically Implantable Neural Probes in the Era of CMOS Neuroelectronics," *Frontiers in Neuroscience* 17 (2023): 1275908.

24. L. Guo, "The Pursuit of Chronically Reliable Neural Interfaces: A Materials Perspective," *Frontiers in Neuroscience* 10 (2016): 599, https://doi.org/10.3389/fnins.2016.00599.

25. Y. Liu, Z. Liu, Y. Zhou, and Y. Tian, "Implantable Electrochemical Sensors for Brain Research," *JACS Au* 3, no. 6 (2023): 1572–1582, https://doi.org/10.1021/jacsau.3c00200.

26. M. Nimgampalle, H. Chakravarthy, S. Sharma, et al., "Neurotransmitter Systems in the Etiology of Major Neurological Disorders: Emerging Insights and Therapeutic Implications," *Ageing Research Reviews* 89 (2023): 101994, https://doi.org/10.1016/j.arr.2023.101994.

27. K. B. Mirza, C. T. Golden, K. Nikolic, and C. Toumazou, "Closed-Loop Implantable Therapeutic Neuromodulation Systems Based on Neurochemical Monitoring," *Frontiers in Neuroscience* 13 (2019): 808, https://doi.org/10.3389/fnins.2019.00808.

28. S. M. Won, L. Cai, P. Gutruf, and J. A. Rogers, "Wireless and Battery-Free Technologies for Neuroengineering," *Nature Biomedical Engineering* 7, no. 4 (2023): 405–423, https://doi.org/10.1038/s41551-021-00683-3.

29. X. Cui, L. Wu, C. Zhang, and Z. Li, "Implantable Self-Powered Systems for Electrical Stimulation Medical Devices," *Advanced Science (Weinh)* 12, no. 24 (2025): 2412044.

30. M. Vöröslakos, K. Kim, N. Slager, et al., "HectoSTAR µLED Optoelectrodes for Large-Scale, High-Precision in Vivo Opto-Electrophysiology," *Advanced Science* 9, no. 18 (2022): 2105414.

31. A. Lakunina, K. Z. Socha, A. Ladd, et al., "Neuropixels Opto: Combining High-Resolution Electrophysiology and Optogenetics," *BioRxiv* (2025).

32. B. Spagnolo, A. Balena, R. T. Peixoto, et al., "Tapered Fibertrodes for Optoelectrical Neural Interfacing in Small Brain Volumes With Reduced Artefacts," *Nature Materials* 21, no. 7 (2022): 826–835, https://doi.org/10.1038/s41563-022-01272-8.

33. S. Lee, M. K. Kim, S. Kwon, et al., "Advanced Micro-OLED Integration on Thin and Flexible Polymer Neural Probes for Targeted Optogenetic Stimulation," *Advanced Functional Materials* 35 (2025): 2420758, https://doi.org/10.1002/adfm.202420758.

34. A. Canales, S. Park, A. Kilias, and P. Anikeeva, "Multifunctional Fibers as Tools for Neuroscience and Neuroengineering," *Accounts of Chemical Research* 51, no. 4 (2018): 829–838, https://doi.org/10.1021/acs.accounts.7b00558.

35. K. Xie, N. Wang, X. Lin, et al., "Organic Electrochemical Transistor Arrays for Real-Time Mapping of Evoked Neurotransmitter Release In Vivo," *Elife* 9 (2020): 50345, https://doi.org/10.7554/eLife.50345.

36. D. Zheng, F. Pisano, L. Collard, et al., "Toward Plasmonic Neural Probes: SERS Detection of Neurotransmitters Through Gold-Nanoislands-Decorated Tapered Optical Fibers With Sub-10 Nm Gaps," *Advanced Materials* 35, no. 11 (2023): 2200902.

37. G. Buzsáki, E. Stark, A. Berényi, et al., "Tools for Probing Local Circuits: High-Density Silicon Probes Combined With Optogenetics," *Neuron* 86, no. 1 (2015): 92–105, https://doi.org/10.1016/j.neuron.2015.01.028.

38. N. A. Steinmetz, C. Aydin, A. Lebedeva, et al., "Neuropixels 2.0: A Miniaturized High-Density Probe for Stable, Long-Term Brain Recordings," *Science* 372, no. 6539 (2021): abf4588.

39. F. Chen, J. Bian, J. Hu, et al., "Mass Transfer Techniques for Large-Scale and High-Density microLED Arrays," *International Journal of Extreme Manufacturing* 4, no. 4 (2022): 042005, https://doi.org/10.1088/2631-7990/ac92ee.

40. D. Chen, Y.-C. Chen, G. Zeng, D. W. Zhang, and H.-L. Lu, "Integration Technology of Micro-LED for Next-Generation Display," *Research (Wash D C)* 6 (2023): 0047.

41. J. G. McCall, T.-I. Kim, G. Shin, et al., "Fabrication and Application of Flexible, Multimodal Light-Emitting Devices for Wireless Optogenetics," *Nature Protocols* 8, no. 12 (2013): 2413–2428, https://doi.org/10.1038/nprot.2013.158.

42. F. Wu, E. Stark, P.-C. Ku, K. D. Wise, G. Buzsáki, and E. Yoon, "Monolithically Integrated μLEDs on Silicon Neural Probes for High-Resolution Optogenetic Studies in Behaving Animals," *Neuron* 88, no. 6 (2015): 1136–1148, https://doi.org/10.1016/j.neuron.2015.10.032.

43. D. Mao, F. Sun, B. Driscoll, Z. Li, and G. Xu, "Close-Packed Dual-Color Micro-LEDs Enable Cortical-Layer-Specific Bidirectional In VivoOptogenetic Electrophysiology," *Cell Reports Physical Science* 4, no. 12 (2023): 101702.

44. A. J. Taal, C. Lee, J. Choi, B. Hellenkamp, and K. L. Shepard, "Toward Implantable Devices for Angle-Sensitive, Lens-Less, Multifluorescent, Single-Photon Lifetime Imaging in the Brain using Fabry–Perot and Absorptive Color Filters," *Light: Science & Applications* 11, no. 1 (2022): 24, https://doi.org/10.1038/s41377-022-00708-9.

45. A. J. Taal, I. Uguz, S. Hillebrandt, et al., "Optogenetic Stimulation Probes With Single-neuron Resolution Based on Organic LEDs Monolithically Integrated on CMOS," *Nature Electronics* 6, no. 9 (2023): 669–679, https://doi.org/10.1038/s41928-023-01013-y.

46. N. McAlinden, D. Massoubre, E. Richardson, et al., "Thermal and Optical Characterization of Micro-LED Probes for in Vivo Optogenetic Neural Stimulation," *Optics Letters* 38, no. 6 (2013): 992–994, https://doi.org/10.1364/OL.38.000992.

47. W. D. Sacher, X. Luo, Y. Yang, et al., "Visible-Light Silicon Nitride Waveguide Devices and Implantable Neurophotonic Probes on Thinned 200 Mm Silicon Wafers," *Optics Express* 27, no. 26 (2019): 37400–37418, https://doi.org/10.1364/OE.27.037400.

48. T. Xue, A. Stalmashonak, F.-D. Chen, et al., "Implantable Photonic Neural Probes With Out-of-Plane Focusing Grating Emitters," *Scientific Reports* 14, no. 1 (2024): 13812, https://doi.org/10.1038/s41598-024-64037-0.

49. F.-D. Chen, A. Sharma, T. Xue, et al., "Implantable Silicon Neural Probes With Nanophotonic Phased Arrays for Single-lobe Beam Steering," *Communications Engineering* 3, no. 1 (2024): 182, https://doi.org/10.1038/s44172-024-00328-8.

50. T. D. Kozai and A. L. Vazquez, "Photoelectric Artefact From Optogenetics and Imaging on Microelectrodes and Bioelectronics: New Challenges and Opportunities," *Journal of Materials Chemistry B* 3, no. 25 (2015): 4965–4978, https://doi.org/10.1039/C5TB00108K.

51. D. Eriksson, A. Schneider, A. Thirumalai, et al., "Multichannel Optogenetics Combined With Laminar Recordings for Ultra-Controlled Neuronal Interrogation," *Nature Communications* 13, no. 1 (2022): 985, https://doi.org/10.1038/s41467-022-28629-6.

52. Y. Wang, Y. Li, X. Yang, X. Wu, Y. Wang, and W. Pei, "Analysis of Electromagnetic Interference and Shielding in the μLED Optrode Based on Finite Element Method," *Frontiers in Nanotechnology* 3 (2021): 758484.

53. K. Kim, M. Vöröslakos, J. P. Seymour, K. D. Wise, G. Buzsáki, and E. Yoon, "Artifact-Free and High-Temporal-Resolution in Vivo Opto-Electrophysiology With microLED Optoelectrodes," *Nature Communications* 11, no. 1 (2020): 2063, https://doi.org/10.1038/s41467-020-15769-w.

54. X. Liu, Y. Lu, E. Iseri, Y. Shi, and D. Kuzum, "A Compact Closed-Loop Optogenetics System Based on Artifact-Free Transparent Graphene Electrodes," *Frontiers in Neuroscience* 12 (2018): 132, https://doi.org/10.3389/fnins.2018.00132.

55. B. Ji, C. Ge, Z. Guo, et al., "Flexible and Stretchable Opto-Electric Neural Interface for Low-Noise Electrocorticogram Recordings and Neuromodulation in Vivo," *Biosensors and Bioelectronics* 153 (2020): 112009, https://doi.org/10.1016/j.bios.2020.112009.

56. M. Favaro, B. Jeong, P. N. Ross, et al., "Unravelling the Electrochemical Double Layer by Direct Probing of the Solid/Liquid Interface," *Nature Communications* 7 (2016): 12695, https://doi.org/10.1038/ncomms12695.

57. J. Vierock, S. Rodriguez-Rozada, A. Dieter, et al., "BiPOLES Is an Optogenetic Tool Developed for Bidirectional Dual-Color Control of Neurons," *Nature Communications* 12, no. 1 (2021): 4527, https://doi.org/10.1038/s41467-021-24759-5.

58. E. Ko, M. Vöröslakos, G. Buzsáki, and E. Yoon, "Dual-Color μ-LEDs Integrated Neural Interface for Multi-Control Optogenetic Electrophysiology," BioRxiv (2024): 2024, bioRxiv 2024.07.30.605927, https://doi.org/10.1101/2024.07.30.605927.

59. V. Lanzio, M. Lorenzon, S. Dhuey, C. F. Pirri, A. Lamberti, and S. Cabrini, "Scalable Nanophotonic Neural Probes for Multicolor and on-demand Light Delivery in Brain Tissue," *Nanotechnology* 32, no. 26 (2021): 265201.

60. D. A. Roszko, F.-D. Chen, J. Straguzzi, et al., "Foundry-fabricated Dual-color Nanophotonic Neural Probes for Photostimulation and Electrophysiological Recording," *Neurophotonics* 12, no. 2 (2025): 025002, https://doi.org/10.1117/1.NPh.12.2.025002.

61. A. M. Aravanis, L.-P. Wang, F. Zhang, et al., "An Optical Neural Interface: In Vivo Control of Rodent Motor Cortex With Integrated Fiberoptic and Optogenetic Technology," *Journal of Neural Engineering* 4, no. 3 (2007): S143–S156.

62. S. Royer, B. V. Zemelman, M. Barbic, A. Losonczy, G. Buzsáki, and J. C. Magee, "Multi-array Silicon Probes With Integrated Optical Fibers: Light-assisted Perturbation and Recording of Local Neural Circuits in the Behaving Animal," *European Journal of Neuroscience* 31, no. 12 (2010): 2279–2291.

63. F. Pisanello, G. Mandelbaum, M. Pisanello, et al., "Dynamic Illumination of Spatially Restricted or Large Brain Volumes via a Single Tapered Optical fiber," *Nature Neuroscience* 20, no. 8 (2017): 1180–1188, https://doi.org/10.1038/nn.4591.

64. M. Pisanello, F. Pisano, L. Sileo, et al., "Tailoring Light Delivery for Optogenetics by Modal Demultiplexing in Tapered Optical Fibers," *Scientific Reports* 8, no. 1 (2018): 4467, https://doi.org/10.1038/s41598-018-22790-z.

65. F. Pisano, M. Pisanello, L. Sileo, et al., "Focused Ion Beam Nanomachining of Tapered Optical Fibers for Patterned Light Delivery," *Microelectronic Engineering* 195 (2018): 41–49, https://doi.org/10.1016/j.mee.2018.03.023.

66. A. Balena, M. Bianco, F. Pisano, et al., "Two-photon Fluorescence-assisted Laser Ablation of Non-planar Metal Surfaces: Fabrication of Optical Apertures on Tapered Fibers for Optical Neural Interfaces," *Optics Express* 28, no. 15 (2020): 21368–21381, https://doi.org/10.1364/OE.395187.

67. M. S. Andriani, M. Bianco, C. Montinaro, et al., "Low-NA Two-Photon Lithography Patterning of Metal/Dielectric Tapered Optical Fibers for

Depth-Selective, Volumetric Optical Neural Interfaces," *Optics Express* 32, no. 27 (2024): 48772–48785, https://doi.org/10.1364/OE.541017.

68. A. Balena, M. Bianco, F. Pisanello, and M. De Vittorio, "Recent Advances on High-Speed and Holographic Two-Photon Direct Laser Writing," *Advanced Functional Materials* 33, no. 39 (2023): 2211773, https://doi.org/10.1002/adfm.202211773.

69. A. Balena, M. Bianco, M. S. Andriani, et al., "Fabrication of Nonplanar Tapered Fibers to Integrate Optical and Electrical Signals for Neural Interfaces in Vivo," *Nature Protocols* 20 (2025): 1768–1809, https://doi.org/10.1038/s41596-024-01105-9.

70. A. Tsakas, C. Tselios, D. Ampeliotis, C. T. Politi, and D. Alexandropoulos, "(INVITED)Review of Optical Fiber Technologies for Optogenetics," *Results in Optics* 5 (2021): 100168, https://doi.org/10.1016/j.rio.2021.100168.

71. Y. Wu, B.-Z. Li, L. Wang, et al., "An Unsupervised Real-time Spike Sorting System Based on Optimized OSort," *Journal of Neural Engineering* 20, no. 6 (2023): 066015.

72. N. C. Rogasch, M. Biabani, and T. P. Mutanen, "Designing and Comparing Cleaning Pipelines for TMS-EEG Data: A Theoretical Overview and Practical Example," *Journal of Neuroscience Methods* 371 (2022): 109494, https://doi.org/10.1016/j.jneumeth.2022.109494.

73. Y. Gao, H. Chao, L. Cavuoto, et al., "Deep Learning-Based Motion Artifact Removal in Functional Near-Infrared Spectroscopy," *Neurophotonics* 9, no. 4 (2022): 041406.

74. L.-M. Vortmann, S. Ceh, and F. Putze, "Multimodal EEG and Eye Tracking Feature Fusion Approaches for Attention Classification in Hybrid BCIs," *Frontiers in Computer Science* 4 (2022): 780580.

75. T. Merk, V. Peterson, R. Köhler, S. Haufe, R. M. Richardson, and W.-J. Neumann, "Machine Learning Based Brain Signal Decoding for Intelligent Adaptive Deep Brain Stimulation," *Experimental Neurology* 351 (2022): 113993, https://doi.org/10.1016/j.expneurol.2022.113993.

76. A. Carnicer-Lombarte, S.-T. Chen, G. G. Malliaras, and D. G. Barone, "Foreign Body Reaction to Implanted Biomaterials and Its Impact in Nerve Neuroprosthetics," *Frontiers in Bioengineering and Biotechnology* 9 (2021): 622524, https://doi.org/10.3389/fbioe.2021.622524.

77. V. S. Polikov, P. A. Tresco, and W. M. Reichert, "Response of Brain Tissue to Chronically Implanted Neural Electrodes," *Journal of Neuroscience Methods* 148, no. 1 (2005): 1–18, https://doi.org/10.1016/j.jneumeth.2005.08.015.

78. T. D. Y. Kozai, A. S. Jaquins-Gerstl, A. L. Vazquez, A. C. Michael, and X. T. Cui, "Brain Tissue Responses to Neural Implants Impact Signal Sensitivity and Intervention Strategies," *ACS Chemical Neuroscience* 6, no. 1 (2015): 48–67, https://doi.org/10.1021/cn500256e.

79. A. Lecomte, C. Descamps, and C. Bergaud, "A Review on Mechanical Considerations for Chronically-Implanted Neural Probes," *Journal of Neural Engineering* 15 (2018): 1741–2552.

80. S. F. Owen, M. H. Liu, and A. C. Kreitzer, "Thermal Constraints on In Vivo Optogenetic Manipulations," *Nature Neuroscience* 22, no. 7 (2019): 1061–1065, https://doi.org/10.1038/s41593-019-0422-3.

81. S. Budday, R. Nay, R. de Rooij, et al., "Mechanical Properties of Gray and White Matter Brain Tissue by Indentation," *Journal of the Mechanical Behavior of Biomedical Materials* 46 (2015): 318–330, https://doi.org/10.1016/j.jmbbm.2015.02.024.

82. A. Villamarin-Ortiz, C. F. Reiche, and F. Federer, "Cortical Response to Acute Implantation of the Utah Optrode Array in Macaque Cortex," *Advanced Healthcare Materials* 15, no. 3 (2026): 00575.

83. A. Perna, J. F. Ribeiro, and G. Orban, "Impact of Tip Size and Shape on the Insertion Force of Implantable CMOS Neural Probes," in *2023 11th International IEEE/EMBS Conference on Neural Engineering (NER)* (Baltimore, MD, USA 2023): 1–4, https://doi.org/10.1109/NER52421.2023.10123886.

84. M. H. Malekoshoaraie, B. Wu, D. D. Krahe, et al., "Fully Flexible Implantable Neural Probes for Electrophysiology Recording and Controlled Neurochemical Modulation," *Microsystems & Nanoengineering* 10 (2024): 91, https://doi.org/10.1038/s41378-024-00685-6.

85. S. Lv, Z. Xu, F. Mo, et al., "Long-term stability strategies of deep brain flexible neural interface," *npj Flexible Electronics* 9, no. 1 (2025): 40.

86. S. Guan, J. Wang, X. Gu, et al., "Elastocapillary Self-assembled Neurotassels for Stable Neural Activity Recordings," *Science Advances* 5, no. 3 (2019): aav2842, https://doi.org/10.1126/sciadv.aav2842.

87. H. C. Lee, F. Ejserholm, J. Gaire, et al., "Histological Evaluation of Flexible Neural Implants; Flexibility Limit for Reducing the Tissue Response?," *Journal of Neural Engineering* 14, no. 3 (2017): 036026, https://doi.org/10.1088/1741-2552/aa68f0.

88. W. Lee, M. Moon, H. G. Kim, T. H. Lee, and M. S. Oh, "Heat Stress-induced Memory Impairment Is Associated With Neuroinflammation in Mice," *Journal of Neuroinflammation* 12 (2015): 102.

89. D. Fei, J. Li, Z. Li, X. Dong, H. Yin, and J. Dai, "Thermal Control Study of Miniaturized Implantable Optoelectronic Devices for Neural Stimulation," *Discover Electronics* 2, no. 1 (2025): 85, https://doi.org/10.1007/s44291-025-00117-3.

90. P. Le Floch, S. Zhao, R. Liu, et al., "3D spatiotemporally Scalable In Vivo Neural Probes Based on Fluorinated Elastomers," *Nature Nanotechnology* 19, no. 3 (2024): 319–329, https://doi.org/10.1038/s41565-023-01545-6.

91. M. Tintelott, A. Schander, and W. Lang, "Understanding Electrical Failure of Polyimide-Based Flexible Neural Implants: The Role of Thin Film Adhesion," *Polymers (Basel)* 14, no. 18 (2022): 3702.

92. E. Ko, J. R. L. Ruiz, M. Vöröslakos, M.-L. Hsieh, G. Buzsáki, and E. Yoon, "Flexlite: Flexible Micro-LED Integrated Optoelectrodes for Long-Term Chronic Deep-brain Studies," *BioRxiv* (2024).

93. C. Kant, A. Shukla, S. K. M. McGregor, S.-C. Lo, E. B. Namdas, and M. Katiyar, "Large Area Inkjet-Printed OLED Fabrication With Solution-Processed TADF Ink," *Nature Communications* 14, no. 1 (2023): 7220, https://doi.org/10.1038/s41467-023-43014-7.

94. D. Wang, J. Hauptmann, and C. May, "OLED Manufacturing on Flexible Substrates towards Roll-to-Roll," *MRS Advances* 4, no. 24 (2019): 1367–1375, https://doi.org/10.1557/adv.2019.62.

95. M. Meneghetti, K. Sui, and C. Markos, "Thermally Drawn Optoelectronic and Optofluidic Polymer Fibres for Brain Applications," in *Advanced Optical and Optoelectronic Fibers*, ed. L. Wei, (Springer Nature Singapore, 2024), 75–92.

96. K. Sui, M. Meneghetti, J. Kaur, R. J. F. Sørensen, R. W. Berg, and C. Markos, "Adaptive Polymer fiber Neural Device for Drug Delivery and Enlarged Illumination Angle for Neuromodulation," *Journal of Neural Engineering* 19, no. 1 (2022): 016035, https://doi.org/10.1088/1741-2552/ac5267.

97. I. Richard, A. K. Maurya, S. Shadman, et al., "Unraveling the Influence of Thermal Drawing Parameters on the Microstructure and Thermo–Mechanical Properties of Multimaterial Fibers," *Small* 18, no. 4 (2022): 2101392, https://doi.org/10.1002/smll.202101392.

98. W. Yan, C. Dong, Y. Xiang, et al., "Thermally Drawn Advanced Functional Fibers: New Frontier of Flexible Electronics," *Materials Today* 35 (2020): 168–194, https://doi.org/10.1016/j.mattod.2019.11.006.

99. Y. Kim, Y. Lee, J. Yoo, et al., "Multifunctional and Flexible Neural Probe With Thermally Drawn Fibers for Bidirectional Synaptic Probing in the Brain," *ACS Nano* 18, no. 20 (2024): 13277–13285, https://doi.org/10.1021/acsnano.4c02578.

100. E. A. Kiyatkin, "Brain Temperature and Its Role in Physiology and Pathophysiology: Lessons From 20 Years of Thermorecording," *Temperature* 6, no. 4 (2019): 271–333, https://doi.org/10.1080/23328940.2019.1691896.

101. K. Sui, M. Meneghetti, G. Li, et al., "In Vivo Brain Temperature Mapping Using Polymer Optical fiber Bragg Grating Sensors," *Optics Letters* 48, no. 16 (2023): 4225–4228, https://doi.org/10.1364/OL.498031.

102. Z. Fekete, Á. C. Horváth, and A. Zátonyi, "Infrared Neuromodulation:A Neuroengineering Perspective," *Journal of Neural Engineering* 17, no. 5 (2020): 051003, https://doi.org/10.1088/1741-2552/abb3b2.

103. M. Meneghetti, J. Kaur, K. Sui, J. F. Sørensen, R. W. Berg, and C. Markos, "Soft Monolithic Infrared Neural Interface for Simultaneous Neurostimulation and Electrophysiology," *Light: Science & Applications* 12, no. 1 (2023): 127, https://doi.org/10.1038/s41377-023-01164-9.

104. K. Na, Z. J. Sperry, J. Lu, et al., "Novel Diamond Shuttle to Deliver Flexible Neural Probe With Reduced Tissue Compression," *Microsystems & Nanoengineering* 6, no. 1 (2020): 37, https://doi.org/10.1038/s41378-020-0149-z.

105. K. Srikantharajah, R. Medinaceli Quintela, K. Doerenkamp, et al., "Minimally-Invasive Insertion Strategy and In Vivo Evaluation of Multi-Shank Flexible Intracortical Probes," *Scientific Reports* 11, no. 1 (2021): 18920, https://doi.org/10.1038/s41598-021-97940-x.

106. M. Cerezo-Sanchez, E. McGlynn, S. Bartoletti, et al., "Bioresorbable Insertion Aids for Brain Implantable Flexible Probes: A Comparative Study on Silk Fibroin, Alginate, and Disaccharides," *Advanced NanoBiomed Research* 3, no. 9 (2023): 2200117, https://doi.org/10.1002/anbr.202200117.

107. N. V. Apollo, B. Murphy, K. Prezelski, et al., "Gels, Jets, Mosquitoes, and Magnets: A Review of Implantation Strategies for Soft Neural Probes," *Journal of Neural Engineering* 17, no. 4 (2020): 041002, https://doi.org/10.1088/1741-2552/abacd7.

108. P.-C. Chen, C. G. Young, C. B. Schaffer, and A. Lal, "Ultrasonically Actuated Neural Probes for Reduced Trauma and Inflammation in Mouse Brain," *Microsystems & Nanoengineering* 8, no. 1 (2022): 117, https://doi.org/10.1038/s41378-022-00438-3.

109. W.-J. Hu, J. W. Eaton, T. P. Ugarova, and L. Tang, "Molecular Basis of Biomaterial-Mediated Foreign Body Reactions," *Blood* 98, no. 4 (2001): 1231–1238, https://doi.org/10.1182/blood.V98.4.1231.

110. Y. Lee, H. Shin, D. Lee, S. Choi, I.-J. Cho, and J. Seo, "A Lubricated Nonimmunogenic Neural Probe for Acute Insertion Trauma Minimization and Long-Term Signal Recording," *Adv Sci (Weinh)* 8, no. 15 (2021): 2100231.

111. Y. Choi, W. Jeon, Y. Kim, et al., "Photoinitiated CVD Antifouling Coatings Enable Long-term Stability of Flexible Multifunctional Neural Probes for Chronic Neural Recording," *Biomaterials* 325 (2026): 123554, https://doi.org/10.1016/j.biomaterials.2025.123554.

112. C. Boehler, C. Kleber, N. Martini, et al., "Actively controlled release of Dexamethasone From Neural Microelectrodes in a Chronic In Vivo study," *Biomaterials* 129 (2017): 176–187, https://doi.org/10.1016/j.biomaterials.2017.03.019.

113. X. Gao, H. Wei, W. Ma, et al., "Inflammation-free Electrochemical in Vivo Sensing of Dopamine With Atomic-Level Engineered Antioxidative Single-atom Catalyst," *Nature Communications* 15, no. 1 (2024): 7915, https://doi.org/10.1038/s41467-024-52279-5.

114. L. Luo, F. Zhang, L. Wang, Y. Liu, and J. Leng, "Recent Advances in Shape Memory Polymers: Multifunctional Materials, Multiscale Structures, and Applications," *Advanced Functional Materials* 34, no. 14 (2024): 2312036, https://doi.org/10.1002/adfm.202312036.

115. A. Teixeira do Nascimento, P. R. Stoddart, T. Goris, et al., "Stimuli-Responsive Materials for Biomedical Applications," *Advanced Materials* 37, no. 36 (2025): 07559, https://doi.org/10.1002/adma.202507559.

116. H. J. Reis, C. Guatimosim, M. Paquet, et al., "Neuro-Transmitters in the Central Nervous System & Their Implication in Learning and Memory Processes," *Current Medicinal Chemistry* 16, no. 7 (2009): 796–840.

117. D. Pikor, M. Hurla, B. Slowikowski, et al., "Calcium Ions in the Physiology and Pathology of the Central Nervous System," *International Journal of Molecular Sciences* 25, no. 23 (2024): 13133.

118. M. K. Jha and B. M. Morrison, "Glia-neuron energy metabolism in health and diseases: New insights into the role of nervous system metabolic transporters (1090-2430 (Electronic))," *Experimental Neurology* 309 (2018): 23–31.

119. B. Li and R. D. Freeman, "Neurometabolic Coupling Between Neural Activity, Glucose, and Lactate in Activated Visual Cortex," *Journal of Neurochemistry* 135 (2015): 742–754.

120. A. F. Salvador, K. A. de Lima, and J. Kipnis, "Neuromodulation by the Immune System: A Focus on Cytokines," *Nature Reviews Immunology* 21, no. 8 (2021): 526–541, https://doi.org/10.1038/s41577-021-00508-z.

121. K. W. Scangos, A. N. Khambhati, P. M. Daly, et al., "Closed-loop Neuromodulation in an Individual With Treatment-Resistant Depression," *Nature Medicine* 27, no. 10 (2021): 1696–1700, https://doi.org/10.1038/s41591-021-01480-w.

122. P. Swetha, S. Munusamy, K. S. S. D. Neurotransmitters, and S. Tsujimura, *Overview of Neurotransmitter Detection and Its Importance, in Future Approaches to Electrochemical Sensing of* (Royal Society of Chemistry, 2025).

123. D. Kondziella, "The Top 5 Neurotransmitters From a Clinical Neurologist's Perspective," *Neurochemical Research* 42, no. 6 (2017): 1767–1771, https://doi.org/10.1007/s11064-016-2101-z.

124. J. Y. Lee, M. Mohammadi, and Y. Wang, "Detecting and Differentiating Neurotransmitters Using Ultraviolet Plasmonic Engineered Native Fluorescence," *RSC Advances* 13, no. 46 (2023): 32582–32588, https://doi.org/10.1039/D3RA05405E.

125. H. Wei and E. Wang, "Nanomaterials With Enzyme-Like Characteristics (nanozymes): Next-Generation Artificial Enzymes," *Chemical Society Reviews* 42, no. 14 (2013): 6060–6093, https://doi.org/10.1039/c3cs35486e.

126. A. Stuber and N. Nakatsuka, "Aptamer Renaissance for Neurochemical Biosensing," *ACS Nano* 18, no. 4 (2024): 2552–2563, https://doi.org/10.1021/acsnano.3c09576.

127. C. M. Lewis, C. Boehler, R. Liljemalm, P. Fries, T. Stieglitz, and M. Asplund, "Recording Quality Is Systematically Related to Electrode Impedance," *Advanced Healthcare Materials* 13, no. 24 (2024): 2303401, https://doi.org/10.1002/adhm.202303401.

128. C. Boehler, T. Stieglitz, and M. Asplund, "Nanostructured Platinum Grass Enables Superior Impedance Reduction for Neural Microelectrodes," *Biomaterials* 67 (2015): 346–353, https://doi.org/10.1016/j.biomaterials.2015.07.036.

129. M. Vomero, C. Gueli, and E. Zucchini, "Flexible Bioelectronic Devices Based on Micropatterned Monolithic Carbon Fiber Mats," *Advanced Materials Technologies* 5, no. 2 (2020): 1900713.

130. M. Devi, M. Vomero, E. Fuhrer, et al., "Carbon-Based Neural Electrodes: Promises and Challenges," *Journal of Neural Engineering* 18, no. 4 (2021): 041007, https://doi.org/10.1088/1741-2552/ac1e45.

131. T. Stuart, W. J. Jeang, R. A. Slivicki, et al., "Wireless, Battery-Free Implants for Electrochemical Catecholamine Sensing and Optogenetic Stimulation," *Acs Nano* 17, no. 1 (2023): 561–574, https://doi.org/10.1021/acsnano.2c09475.

132. E. Castagnola, Q. Cao, E. Robbins, et al., "Glassy Carbon Fiber-Like Multielectrode Arrays for Neurochemical Sensing and Electrophysiology Recording," *Advanced Materials Technologies* 10, no. 4 (2025): 2400863, https://doi.org/10.1002/admt.202400863.

133. M. Seiti, A. Giuri, C. E. Corcione, and E. Ferraris, "Advancements in Tailoring PEDOT: PSS Properties for Bioelectronic Applications: A Comprehensive Review," *Biomaterials Advances* 154 (2023): 213655, https://doi.org/10.1016/j.bioadv.2023.213655.

134. J. T. Robinson, C. Xie, E. Pohlmeyer, et al., "Developing Next-Generation Brain Sensing Technologies—A Review," *IEEE Sensors Journal* 19, no. 22 (2019): 10163–10175, https://doi.org/10.1109/JSEN.2019.2931159.

135. S. Carli, M. Bianchi, E. Zucchini, et al., "Electrodeposited PEDOT:Nafion Composite for Neural Recording and Stimulation," *Advanced Healthcare Materials* 8, no. 19 (2019): 1900765, https://doi.org/10.1002/adhm.201900765.

136. B. T. Seaton, D. F. Hill, S. L. Cowen, and M. L. Heien, "Mitigating the Effects of Electrode Biofouling-Induced Impedance for Improved Long-Term Electrochemical Measurements in Vivo," *Analytical Chemistry* 92, no. 9 (2020): 6334–6340, https://doi.org/10.1021/acs.analchem.9b05194.

137. D. Ohayon, V. Druet, and S. Inal, "A Guide for the Characterization of Organic Electrochemical Transistors and Channel Materials," *Chemical Society Reviews* 52, no. 3 (2023): 1001–1023, https://doi.org/10.1039/D2CS00920J.

138. D. Khodagholy, T. Doublet, P. Quilichini, et al., "In Vivo Recordings of Brain Activity Using Organic Transistors," *Nature Communications* 4 (2013): 1575, https://doi.org/10.1038/ncomms2573.

139. R. B. Rashid, X. Ji, and J. Rivnay, "Organic Electrochemical Transistors in Bioelectronic Circuits," *Biosensors and Bioelectronics* 190 (2021): 113461, https://doi.org/10.1016/j.bios.2021.113461.

140. C. Zhao, J. Yang, and W. Ma, "Transient Response and Ionic Dynamics in Organic Electrochemical Transistors," *Nanomicro Letters* 16, no. 1 (2024): 233.

141. J. Harris, M. Brothers, V. Coyle, S. Kim, and E. Ratcliff, "Advancing Ultrasensitive, Drift-Correcting Dual Floating Gate Organic Electrochemical Transistors for Yeast Sensing," *Chemistry of Materials* 36, no. 1 (2024): 324–331, https://doi.org/10.1021/acs.chemmater.3c02164.

142. N. P. Menezes, T. Nicolini, M. Barker, et al., "Improved Stability of Organic Electrochemical Transistor Performance With a Low Swelling Mixed Conducting Polymer: A Comparative Study With PEDOT:PSS," *Journal of Materials Chemistry C* 11, no. 19 (2023): 6296–6300, https://doi.org/10.1039/D3TC00108C.

143. S. Han, A. G. Polyravas, S. Wustoni, S. Inal, and G. G. Malliaras, "Integration of Organic Electrochemical Transistors With Implantable Probes," *Advanced Materials Technologies* 6, no. 12 (2021): 2100763, https://doi.org/10.1002/admt.202100763.

144. P. M. Borden, P. Zhang, A. V. Shivange, et al., "A Fast Genetically Encoded Fluorescent Sensor for Faithful in Vivo Acetylcholine Detection in Mice, Fish, Worms and Flies," *BioRxiv* (2020).

145. N. Tjahjono, Y. Jin, A. Hsu, M. Roukes, and L. Tian, "Letting the Little Light of Mind Shine: Advances and Future Directions in Neurochemical Detection," *Neuroscience Research* 179 (2022): 65–78, https://doi.org/10.1016/j.neures.2021.11.012.

146. F. Pisano, M. Pisanello, S. J. Lee, et al., "Depth-resolved fiber Photometry With a Single Tapered Optical fiber Implant," *Nature Methods* 16, no. 11 (2019): 1185–1192, https://doi.org/10.1038/s41592-019-0581-x.

147. N. Byron and S. Sakata, "Fiber Photometry-based Investigation of Brain Function and Dysfunction," *Neurophotonics* 11, no. 1 (2024): S11502.

148. E. H. Simpson, T. Akam, T. Patriarchi, et al., "Lights, Fiber, Action! A Primer on In Vivo Fiber Photometry," *Neuron* 112, no. 5 (2024): 718–739, https://doi.org/10.1016/j.neuron.2023.11.016.

149. A. A. Patel, N. McAlinden, K. Mathieson, and S. Sakata, "Simultaneous Electrophysiology and Fiber Photometry in Freely Behaving Mice," *Frontiers in Neuroscience* 14 (2020): 148, https://doi.org/10.3389/fnins.2020.00148.

150. N. Driscoll, M.-J. Antonini, T. M. Cannon, et al., "Fiber-based Probes for Electrophysiology, Photometry, Optical and Electrical Stimulation, Drug Delivery, and Fast-Scan Cyclic Voltammetry in Vivo," *BioRxiv* (2024).

151. M. L. Rynes, D. A. Surinach, S. Linn, et al., "Miniaturized Head-Mounted Microscope for Whole-cortex Mesoscale Imaging in Freely Behaving Mice," *Nature Methods* 18, no. 4 (2021): 417–425, https://doi.org/10.1038/s41592-021-01104-8.

152. W. Zong, R. Wu, S. Chen, et al., "Publisher Correction: Miniature Two-Photon Microscopy for Enlarged Field-of-View, Multi-Plane and Long-Term Brain Imaging," *Nature Methods* 18, no. 2 (2021): 220, https://doi.org/10.1038/s41592-021-01066-x.

153. B. Zhou, K. Fan, J. Guo, et al., "Plug-and-Play Fiber-Optic Sensors Based on Engineered Cells for Neurochemical Monitoring at High Specificity in Freely Moving Animals," *Science Advances* 9, no. 22: adg0218, https://doi.org/10.1126/sciadv.adg0218.

154. A. I. Pérez-Jiménez, D. Lyu, Z. Lu, G. Liu, and B. Ren, "Surface-Enhanced Raman Spectroscopy: Benefits, Trade-offs and Future Developments," *Chemical Science* 11, no. 18 (2020): 4563–4577, https://doi.org/10.1039/D0SC00809E.

155. D. Zheng, M. F. Kashif, L. Piscopo, et al., "Tunable Nanoislands Decorated Tapered Optical Fibers Reveal Concurrent Contributions in through-Fiber SERS Detection," *ACS Photonics* 11, no. 9 (2024): 3774–3783, https://doi.org/10.1021/acsphotonics.4c00912.

156. W. Lee, B.-H. Kang, H. Yang, et al., "Spread Spectrum SERS Allows Label-Free Detection of Attomolar Neurotransmitters," *Nature Communications* 12, no. 1 (2021): 159, https://doi.org/10.1038/s41467-020-20413-8.

157. D. Zheng, Y. Li, M. F. Kashif, L. Piscopo, M. De Vittorio, and F. Pisanello, "Nanomaterial-Integrated Fiber Neural Probes for Deep Brain Monitoring and Modulation: Challenges and Opportunities," *Advanced Functional Materials* 36 (2025): 17054.

158. Y. Qi, D. Hu, Y. Jiang, et al., "Recent Progresses in Machine Learning Assisted Raman Spectroscopy," *Advanced Optical Materials* 11, no. 14 (2023): 2203104, https://doi.org/10.1002/adom.202203104.

159. A. Sanchez-Aguilera, M. Masmudi-Martín, A. Navas-Olive, et al., "Machine Learning Identifies Experimental Brain Metastasis Subtypes Based on Their Influence on Neural Circuits," *Cancer Cell* 41 (2023): 1637–1649.